Linear Copolymers of Ethylene and Polar Vinyl Monomers via Olefin Metathesis−Hydrogenation: Synthesis, Characterization, and Comparison to Branched Analogues

Stephen E. Lehman, Jr.,[†,§] Kenneth B. Wagener,[*,†] Lisa Saunders Baugh,[*,‡] Steven P. Rucker,[‡] Donald N. Schulz,[‡] Manika Varma-Nair,[‡] and Enock Berluche[‡]

The George and Josephine Butler Polymer Research Laboratory, Department of Chemistry, University of Florida, Gainesville, Florida 32611-7200, and ExxonMobil Research & Engineering Company, Corporate Strategic Research Laboratory, 1545 Route 22 East, Annandale, New Jersey 08801

Received January 11, 2007; Revised Manuscript Received January 29, 2007

ABSTRACT: Materials structurally equivalent to copolymers of ethylene and <10 mol % of vinyl alcohol, vinyl acetate, methyl acrylate, *tert*-butyl acrylate, and acrylic acid were synthesized via ruthenium-catalyzed olefin metathesis copolymerization followed by polymer hydrogenation. These polymers differ from previous metathesis-derived linear polyethylene analogues in that they do not have precise sequence distributions, and therefore, they serve as superior models for chain-addition functional polyethylenes. The ester group-substituted polymers display rapid decreases in melting temperature and heat of fusion with increasing comonomer contents irrespective of the identity of the functional group, consistent with these groups being equally excluded from the crystal lattice. The alcohol-substituted polymers, however, show higher melting temperatures and a weaker property dependence on comonomer content as compared to the other polymers. Thus, the behavior of alkyl branch-free functionalized polyethylenes is consistent with the large body of work involving the effects of functional substituents on polyethylenes containing alkyl branches.

Introduction

Polyethylene (PE) is produced in the highest volume of all synthetic plastics and is considered a class of polymers rather than a single material. The physical properties of polyethylenes can be widely varied by manipulating their microstructural parameters, in particular, the length and placement of alkyl branches along the chain. Another important strategy is the introduction of polar (heteroatom-containing) functionalities via copolymerization or post-functionalization. Polar groups can be used to enhance properties such as toughness, flexibility, impact strength, crack resistance, gas impermeability, adhesion, paintability, and miscibility.[1,2]

Copolymers of ethylene and "polar vinyl" monomers (those with a functional group attached directly to the polymerizing olefin) are traditionally prepared by free-radical polymerization processes similar to those used to make low-density polyethylene (LDPE). LDPEs containing vinyl acetate, alkyl acrylates, acrylic acids, acrylate salts, and vinyl alcohol (from vinyl acetate hydrolysis) are used commercially as barrier films, adhesives, pipes and tubes, and high-toughness molding resins. However, the reactivity differences between ethylene and many polar vinyl monomers in free-radical polymerization are large, such that only limited ranges of copolymer compositions are available, and very little control of microstructure and comonomer sequence distribution can be achieved.[2] The base material properties of these copolymers are also limited by the many short-chain alkyl branches (SCBs) introduced by the free-radical polymerization mechanism.[2,3]

* Corresponding author. E-mail: wagener@chem.ufl.edu; lisa.s.baugh@exxonmobil.com.
† University of Florida.
‡ ExxonMobil Research & Engineering Company.
§ Current address: SDC Materials, 940 South Park Lane, Suite 2, Tempe, Arizona 85281. E-mail: ed.lehman@sdcmaterials.com.

Ethylene/polar vinyl copolymers with low branch content—functional versions of high-density polyethylene (HDPE)—are a target of great commercial interest. At low polar comonomer contents, the desirable material properties of HDPE, including high tensile strength, stiffness, and low-temperature impact strength,[4] are expected to be retained while adding the benefits of polar functionalities. Much recent effort has been directed toward the development of transition metal catalyst systems capable of making functional HDPE-like materials via coordination−insertion copolymerization of ethylene and polar vinyl monomers.[1,5] Such processes would theoretically provide much greater control of chain microstructure and linearity than free-radical polymerization. However, the metal-mediated olefin/polar vinyl copolymerization systems developed to date exhibit numerous limitations. These include hyperbranching, low copolymer molecular weights, the need for a spacer group separating the polar functionality and the polymerizing olefin, compositional restriction to either very low or very high polar comonomer contents, and the placement of polar groups predominantly at chain ends.

Currently, the only general method of synthesizing linear polyethylenes with low to moderate amounts of in-chain polar vinyl comonomer incorporation is olefin metathesis polymerization, which produces functional polyalkenamers that can be transformed into model ethylene/polar vinyl copolymers by hydrogenation. Ring-opening metathesis polymerization (ROMP) of functionalized cycloalkenes with polar-tolerant Ru catalysts is a common route into these materials (Scheme 1). Homopolymerizations of cyclooctenes bearing halide and oxygenated substituents in the 5-position have been carried out by several groups; hydrogenation of these materials gives polymers formally containing 25 mol % of the analogous polar vinyl comonomers.[6−8] The functionality-bearing backbone carbons are separated by a run length of *r* methylene groups where *r* equals 6, 7, or 8 carbons depending on monomer regioaddition.

10.1021/ma070085p CCC: $37.00
Published on Web 03/24/2007

Scheme 1. Sequential ROMP Homopolymerization/Hydrogenation of 5-Substituted Cyclooctenes (R = Functional Group) Producing Polyethylenes Having Run Lengths of Six (Head-to-Head, HH), Seven (Head-to-Tail, HT), and Eight (Tail-to-Tail, TT) Methylene Units between Substituents

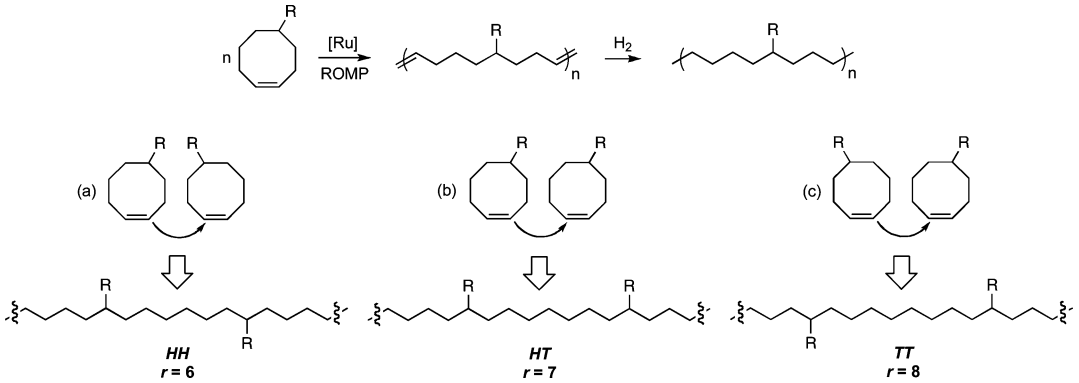

Scheme 2. Synthesis of Polyethylenes Having "Precise" Branch Placement via Sequential ADMET Homopolymerization/ Hydrogenation (R = Functional Group)

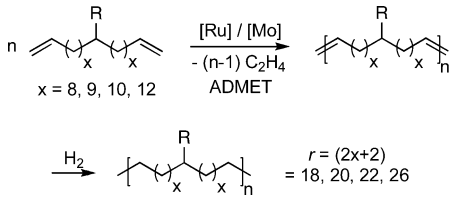

Similarly, ROMP/hydrogenation of 1,2-difunctionalized cycloalkenes has been employed to model polyethylenes with high contents of regio- and stereoregular alcohol and amine substituents.[6c,9] The post-polymerization functionalization of polyalkenamers by Rh-catalyzed hydroformylation,[6b] and of polyalkenamers and borane-substituted cyclooctene monomers by hydroboration/oxidation,[10] have also been used to prepare linear functional polyethylene analogues with varying polar contents. The Wagener group has developed a versatile strategy utilizing acyclic diene metathesis polymerization (ADMET) of symmetrically substituted α,ω-dienes to make model polyolefins bearing a wide range of substituents at precise intervals along the chain (Scheme 2).[11] The low polar content functional polyethylenes obtained through this method have compositions equivalent to 7−11 mol % polar comonomer incorporation and methylene run lengths of $r = 18$, 20, 22, or 26.

Despite their utility, metathesis homopolymerization/hydrogenation techniques are not ideally suited for modeling "real" chain-addition functional polyolefins. The preparation of linear polyethylenes having small polar vinyl monomer contents by this route would require impractically large functional monomers. More importantly, the exclusively short and/or precise run lengths in the products are not analogous to the sequence distributions present in chain-addition polyethylenes. Chain-addition copolymers can contain very long run lengths and broad run length distributions, even at high comonomer contents, which play a major role in controlling crystallinity and physical properties. Furthermore, even at relatively long run lengths, the regular structures of "precisely" branched ADMET copolymers exert unique influences on solid-state structure and produce unusual thermal behavior.[11b−e,i−l,n,o,12]

Recently, we have used the ADMET *copolymerization* of methyl-substituted and linear α,ω-dienes to prepare model ethylene/propylene (EP) copolymers having both lower comonomer contents ($\geq$0.3 mol % propylene) and more randomly placed substituents than available via metathesis homopolymerization.[13] Due to their longer methylene run lengths and broader run length distributions as compared to "precise" ADMET EPs, these "random" materials exhibit thermal behavior more similar to true chain-addition copolymers. Hiltner and Rowan et al. have similarly employed ROMP copolymerization of cyclooctene and 5-chlorocyclooctene to construct linear models for "random" poly(ethylene/vinyl chloride)s.[6e−g]

Herein, we report the use of metathesis copolymerization to synthesize a suite of *HDPE-like, low-polar-content, rigorously linear "random" functional polyethylenes*. Both ROMP copolymerization of cyclooctene with functional cyclooctenes and ADMET copolymerization of 1,9-decadiene with functional α,ω-dienes were used to construct copolymers formally containing 1.9−8.3 mol % of vinyl acetate (VAC), vinyl alcohol (VOH), acrylic acid (AA), methyl acrylate (MA), or *tert*-butyl acrylate (TBA) comonomer units. The long, nonprecise methylene run lengths in these materials, in conjunction with the absence of any alkyl branches, render them improved models for studying the fundamental structure−property effects of polar substituents on the bulk properties of polyethylenes.

Experimental Section

Materials. Air- and moisture-sensitive reactions were conducted using standard Schlenk techniques under argon. Bis(tricyclohexylphosphine)benzylidene Ru(IV) dichloride ($RuCl_2(PCy_3)_2CHPh$, **Ru-1**) was obtained from Fluka or Materia. $(Ph_3P)_3RhCl$ (Wilkinson's catalyst) was obtained from Strem. H_2 and CO were obtained from Matheson. Ethyl vinyl ether was purchased pre-stabilized with KOH from Aldrich Chemical Co. Ethylidene[1,3-dimesitylimidazolidin-2-ylidene](tricyclohexylphosphine)Ru(IV) dichloride ($RuCl_2(SIMes)(PCy_3)CHCH_3$, **Ru-3**),[14] 3-methylbut-2-ene-1-ylidene[1,3-dimesitylimidazolidin-2-ylidene](tricyclohexylphosphine)Ru(IV) dichloride ($RuCl_2(SIMes)(PCy_3)CHCH{=}C(CH_3)_2$, **Ru-4**),[15] and dodec-11-enoic acid[11c] were synthesized according to literature procedures. Free-radical copolymers were obtained from Aldrich Chemical Co. (EMA, EAA, EVAC), Monomer−Polymer Dajac Labs (EAA), or ExxonMobil Chemical Co. (EVAC, EMA, EAA). The following materials were purified before use by distillation from CaH_2 (at the noted temperature and pressure) and degassing via freeze−pump−thaw cycles: 1,9-decadiene, 11-bromo-1-undecene, **5** (105−108 °C/100 Torr), **6** (95 °C/100 Torr), 1,3-dimethyl-3,4,5,6-tetrahydro-2(1*H*)-pyrimidinone (DMPU, 135 °C/~40 Torr; stored in a Schlenk tube over activated 3 Å molecular sieves), and cyclooctene (Aldrich Chemical Co., 95% purity with balance cyclooctane; molar amounts were corrected for purity as given by the supplier or determined by ^{1}H nuclear magnetic resonance (NMR) spectroscopy or gas chromatography (GC)). 10-Undecenal was purified by vacuum distillation from Na_2SO_4 and stored over molecular sieves in a refrigerator. Ru catalysts were stored in a dry box; small aliquots were periodically removed and stored in a desiccator for use in copolymerizations assembled under atmospheric conditions. Toluene-d_8 for kinetics experiments was distilled and degassed by three freeze−pump−thaw cycles. 2,6-Di-*tert*-butyl-

4-methylphenol (butylated hydroxytoluene, BHT) was optionally sublimed before use. $CeCl_3$ was prepared by drying $CeCl_3{\bullet}(H_2O)_7$ under vacuum overnight at 140 °C.[16] *o*-Dichlorobenzene (ODCB), 1,1,2,2-tetrachloroethane (TCE), xylenes, and all other materials were either purchased from commercial sources and used as received or prepared as described in the Supporting Information.

General Characterization. Infrared (IR) spectra were collected on Bruker 200, Mattson Galaxy Series 5000, or Mattson Polaris spectrometers. Monomers and polymeric oils were analyzed as neat thin films on NaCl plates; solid polymers were cast as thin films onto NaCl plates by slow evaporation of a TCE solution at ~130 °C in a covered Petri dish. Solution ^1H and ^{13}C NMR spectroscopy of polyalkenamers and monomers were conducted at room temperature or 50 °C (for some polyalkenamers) using Varian Gemini 300, VXR 300, Mercury 300, Unity Inova 300, UnityPlus 500, or Inova 500 MHz spectrometers. Fast atom bombardment and electrospray ionization high-resolution mass spectrometry (HRMS−FAB and HRMS-EI) were conducted using a FINNIGAN MAT95 Q instrument. Elemental analyses were conducted by Atlantic Microlab (Norcross, GA). Stage melting point (MP) data were determined visually in capillary tubes using a Thomas Hoover oil bath apparatus.

Representative ADMET Procedure. Functionalized diene monomer was placed in a 50 mL Schlenk tube and degassed with stirring overnight under high vacuum (~5×10^{-4} Torr) at 25−40 °C (for **3**, degassing was optimally conducted at 55−60 °C to effect melting). The tube was placed under argon and the desired amount of 1,9-decadiene was added by syringe. The warm solution was shaken to mix the two monomers. Separately, in the drybox, a 500 mL, 3-necked 24/40 round-bottom flask was charged with the appropriate amount of solid Ru catalyst and fitted with two rubber septa and a vacuum adapter. The flask was placed under argon on a Schlenk line. The center joint septum was replaced with an oven-dried shaft (Teflon or polished glass) and blade (Teflon, manually cut to fit the contour of the flask) and attached via a flexible connector to a high-viscosity Arrow 350 mechanical stirrer, and stirring was initiated. The liquid diene mixture was added to the flask via cannula to give a purplish-brown solution, and the contents of the flask were heated to 60−70 °C using an oil bath. After a few hours of stirring under argon, the polymerization was placed under dynamic high vacuum, and outgassing of ethylene was observed. The polymerization was stirred at 55−70 °C for several days under dynamic vacuum during the day and under argon at night (to exclude the possibility of vacuum leaks while unattended). Isolation of the product polyalkenamer was performed according to the appropriate hydrogenation procedure.

Representative ROMP Procedure. Cyclooctene was mixed with the desired amount of the functionalized cyclooctene monomer under atmospheric conditions to form a solution, a measured portion of which was added to a dry, argon-purged 500 mL 3-necked round-bottom flask fitted with an argon inlet, high-viscosity mechanical stirrer apparatus, and septum. ODCB was added to give a solution of the desired concentration, stirring was initiated, and argon was bubbled through the solution for 0.5 h, after which the stirred solution was heated under argon to 60 °C using an oil bath (some polymers were prepared at room temperature). The appropriate amount of Ru catalyst dissolved in a small volume of ODCB was added via syringe, and the polymerization was stirred at 60 °C (or RT) under argon for the desired time period [alternately, the catalyst was dissolved in the total desired volume of predegassed ODCB, and the monomer mixture was added directly]. Subsequently, a quantity of BHT equivalent to 0.05−0.1 wt % of the theoretical polymer yield was added to the solution as a solid. A small quantity (~0.5 mL) of the polymer solution was typically removed by pipet and added to stirred methanol (50 mL) at room temperature to precipitate a portion of the unsaturated polymer, which was isolated by filtration and dried under vacuum overnight at room temperature.

Hydrogenation Procedure 1. After removal of an aliquot of polyalkenamer for characterization (dissolved in hot toluene and precipitated into room-temperature methanol), the polymerization mixture was dissolved in 150 mL reagent grade xylenes at 60 °C and transferred to a glass-lined 450 mL stainless steel Parr reactor containing 15 g chromatographic silica. This stirred mixture was hydrogenated at 90 °C and 500 psig H_2 for 7 days (the reactor was pressurized to 500 psig H_2 and released three times before the final H_2 charge). Subsequently, the reactor was vented and the contents of the glass sleeve were reheated to boil, and filtered to remove the brown silica−Ru catalyst residue through a coarse glass frit funnel preheated with boiling xylenes. The filtrate was heated to boil and precipitated into 700 mL acidified (1 N HCl) isopropyl alcohol at room temperature. The polymer was collected by filtration and reprecipitated from hot xylenes into 700 mL of acidified (1 N HCl) methanol, washed twice by stirring in 250 mL of boiling methanol, and dried under vacuum overnight to give the polymer in 40−70% yield (for the combined polymerization/hydrogenation).

Hydrogenation Procedure 2. The polymerization mixture was cooled, exposed to air, and treated with ethyl vinyl ether (10 mL) for 10 min to deactivate the Ru catalyst. The mixture was subjected to vacuum to remove the ethyl vinyl ether, cooled to 0 °C to facilitate polymer solidification, and subsequently dissolved in 100 mL of toluene (stirring overnight at room temperature to facilitate complete dissolution). Neutral alumina (~2 g, 150 mesh) was added to absorb the catalyst. This mixture was filtered, concentrated, and precipitated into an excess (typically 700 mL) of acidified (1 N HCl) methanol. The unsaturated polymer was collected and dried overnight under vacuum at 60 °C. The unsaturated polymer was then dissolved in 150 mL of stirred xylenes in a glass sleeve for a 450 or 300 mL Parr reactor at 120 °C. Wilkinson's catalyst (100 mg unless otherwise specified) was added, the Parr reactor was assembled, and air was purged by three cycles of pressurization to 500 psig and release. The polymer was then hydrogenated at 120 °C and 500 psig H_2 for 3−7 days, after which the reactor was cooled and depressurized. The polymer in the sleeve was then redissolved by heating to 100−120 °C, precipitated into an excess (700−1000 mL) of acidified (1 N HCl) methanol at 40 °C, collected by filtration, and redissolved/reprecipitated from fresh hot xylenes into 40 °C acidified methanol. The purified polymer was dried in a vacuum oven at 40 °C overnight and obtained in 70−90% yield (for the combined polymerization/hydrogenation).

Hydrogenation Procedure 3. The polymerization solution was poured into a glass sleeve for a 450 mL stainless steel mechanically stirred Parr reactor. ODCB (100 mL) was then layered onto the polymer solution. The layered mixture was not initially stirred in order to prevent any ill effects of dilution (i.e., molecular weight reduction via backbiting reactions). The reactor was assembled and sealed, and three cycles of pressurization to 400 psig H_2 followed by release were performed to expel air. The reactor was then pressurized to 400 psig H_2 and heated to 130 °C. Stirring was initiated when the reactor temperature reached 100 °C. After 24 h (the progress of hydrogenation can be monitored[13] by loss of the sharp medium-intensity out-of-plane alkene C−H bend IR band near 967 cm^{-1}), the solution was cooled and the pressure was released. The glass sleeve was removed, a magnetic stirbar was added, and the mixture was heated in an oil bath to 130−180 °C to redissolve the polymer, which was then precipitated into 700 mL of methanol in a blender. The crushed polymer was collected by filtration, rapidly stirred twice for 5 min in 300 mL boiling methanol, recollected by filtration, and dried under high vacuum at room temperature overnight to give the saturated polymer. Yields were typically 60−80% over the two-step polymerization/hydrogenation procedure, with some portion of the mass loss due to the removal of polyalkenamer aliquots and residues left on surfaces during redissolution and precipitation steps.

Hydrogenation Procedure 4. The polymerization solution was quenched by addition of 0.5 mL of ethyl vinyl ether and 0.1 mL of pyridine, and slowly diluted with 100 mL of ODCB while stirring. A color change from pale orange to bright yellow occurred over several minutes. The solution was then added to 700 mL of methanol in a blender, and the resulting precipitated polymer was collected by filtration, washed twice with 300 mL of clean methanol, and dried overnight under high vacuum at room temperature. The

polymer was then combined with a 5-fold molar excess of *p*-toluenesulfonhydrazide ($TsNHNH_2$) in a large (3 L) round-bottom flask fitted with a reflux condenser and stirbar. The oversized flask is required due to excessive foaming that occurs during the reaction. Xylenes were added in sufficient quantity to make a 2−6 w/v % polymer solution based on the theoretical yield of polymer. This mixture was then degassed by three freeze−pump−thaw cycles and stirred for 4 h at reflux. The hot mixture was then slowly poured into excess methanol (≥10 × volume). The solid polymer was collected by filtration, washed twice with 300 mL of boiling methanol, and dried under high vacuum overnight at room temperature. Yields for polymerization/hydrogenation were typically between 70 and 90%.

Copolymer NMR Analysis. Solution ^{13}C NMR of saturated copolymers was carried out in TCE-d_2 or ODCB-d_4 at 120 °C using a Unity Inova 300 MHz spectrometer equipped with a 10 mm broadband probe and calibrated to the peak for linear PE CH_2 segments at 29.98 ppm. Chromium *tris*-acetylacetonate, $Cr(acac)_3$, was added as a relaxation agent at a concentration of 15 mg/mL (except for linear EAA copolymers). ^1H NMR of hydrogenated copolymers was conducted under similar conditions without relaxation agent, using a UnityPlus 500 MHz instrument equipped with a 5 mm switchable probe. Solid-state ^{13}C NMR (1pda Bloch decay and cp4 cross-polarization) was conducted with a Varian CMX-200 instrument equipped with a 4 mm pencil probe, using a rotor spinning speed of 8 kHz. Copolymer mol % composition was typically calculated using the average of ^1H and ^{13}C NMR measurements as described in the Supporting Information. Representative characterization data for hydrogenated ROMP copolymers are given below. No evidence of residual unsaturation or alkyl branching was observed by ^1H or ^{13}C NMR. Some ADMET and ROMP copolymers showed ^1H NMR end group peaks at 0.92−0.84 (t, CH_3) ppm; some ADMET copolymers also exhibited ^{13}C NMR end group peaks at 32.2 ($CH_2CH_2CH_3$), 29.6 ($CH_2CH_2CH_2CH_3$), 22.9 (CH_2CH_3), and 14.2 (CH_3) ppm.

Poly(ethylene-*co*-vinyl alcohol) (EVOH). ^1H NMR (500 MHz, ODCB-d_4, 120 °C): δ 3.66−3.50 (br, C*H*OH), 2.36−2.25 (t, $CH_2C{=}O$, when present), 1.75−0.95 (m, CH_2). ^{13}C NMR (75 MHz, TCE-d_2, 120 °C): δ 210.84 (C═O, when present), 72.41 (*C*HOH), 43.10 ($CH_2C{=}O$, when present), 38.05 (CH_2CHOH), 29.98 (CH_2), 25.99 (CH_2CH_2CHOH), 24.42 ($CH_2CH_2C{=}O$, when present). IR: 3410 (υ_{O-H}), 2918, 2850, 1718 ($\upsilon_{C=O}$, when present), 1473, 1463, 910, 730, 720 cm^{-1}.

Poly(ethylene-*co*-vinyl acetate) (EVAC). ^1H NMR (500 MHz, ODCB-d_4, 120 °C): δ 5.3−4.7 (br, C*H*O_2CMe), 2.06−1.90 (s, O_2C*Me*), 1.75−0.95 (m, CH_2). ^{13}C NMR (75 MHz, TCE-d_2, 120 °C): δ 170.68 (*C*═O), 34.57 (CH_2CHO_2CMe), 29.98 (CH_2), 25.66 ($CH_2CH_2CHO_2CMe$), 21.38 (O_2C*Me*); *C*HO_2CMe resonance hidden under solvent peak at 74.8−74.1 ppm. IR: 2918, 2850, 1741 ($\upsilon_{C=O}$), 1473, 1463, 1370, 1241, 1020, 730, 720 cm^{-1}.

Poly(ethylene-*co*-methyl acrylate) (EMA). ^1H NMR (500 MHz, ODCB-d_4, 120 °C): δ 3.9−3.5 (s, CO_2*Me*), 2.5−2.3 (m, C*H*CO_2Me), 1.8−1.6 and 1.6−1.4 (m, CH_2CHCO_2Me), 1.5−1.1 (m, CH_2). ^{13}C NMR (75 MHz, ODCB-d_4, 120 °C): δ 175.93 (*C*═O), 50.71 (CO_2*Me*), 45.94 (*C*HCO_2Me), 32.73 (CH_2CHCO_2Me), 29.98 (CH_2), 27.77 ($CH_2CH_2CHCO_2Me$). IR: 2918, 2850, 1738 ($\upsilon_{C=O}$), 1473, 1463, 1194, 1164, 730, 720 cm^{-1}.

Poly(ethylene-*co*-acrylic acid) (EAA). ^1H NMR (500 MHz, ODCB-d_4, 120 °C): δ 2.6−2.4 (br, C*H*CO_2H), 2.0−1.05 (m, CH_2). ^{13}C NMR (75 MHz, TCE-d_2, 120 °C, no $Cr(acac)_3$): δ 179.95 (br, *C*═O), 45.37 (br, *C*HCO_2H), 32.53 (CH_2CHCO_2H), 29.98 (CH_2), 27.69 ($CH_2CH_2CHCO_2H$). IR: 2918, 2850, 1706 ($\upsilon_{C=O}$), 1473, 1463, 1370, 1241, 1020, 730, 720 cm^{-1} (O−H stretch not assigned due to weakness). ^{13}C NMR (solid-state Bloch decay, 50 MHz): δ 183.8 (*C*═O), 47.9 and 44.9 (*C*HCO_2H), 33.3 and 30.9 (overlapping, CH_2), 14.8 (CH_3 end groups).

Poly(ethylene-*co*-*t*-butyl acrylate) (ETBA). ^1H NMR (500 MHz, ODCB-d_4, 120 °C): δ 2.5−2.2 (br, C*H*CO_2CMe_3), 1.9−0.95 (m, CH_2), 1.47 (s, C*Me*$_3$). ^{13}C NMR (125 MHz, TCE-d_2, 120 °C): δ 175.78 (*C*═O), 79.83 (CO_2CMe_3), 46.89 (*C*HCO_2CMe_3), 32.89 ($CH_2CHCO_2CMe_3$), 29.98 (CH_2), 28.66 (C*Me*$_3$), 27.69 ($CH_2CH_2CHCO_2CMe_3$). IR: 2918, 2850, 1729 ($\upsilon_{C=O}$), 1473, 1463, 1366, 1150, 730, 720 cm^{-1}.

Copolymer Molecular Weight Analysis. Gel permeation chromatography (GPC) and light scattering (GPC−LS) copolymer molecular weights reported vs polystyrene (PS) were determined in THF using a 1.0 L/min flow rate with either (a) a Waters Associates GPC equipped with three Polymer Laboratories mixed bed Type D columns and an internal differential refractive index (DRI) detector at 30 °C (typical sample concentration 2.5 mg/mL) or (b) a Waters Associates GPCV2000 equipped with two Waters Styragel HR-5E columns, internal DRI and differential viscosity (DP) detectors, and a Precision two-angle light scattering (LS) detector collecting at 15° (operated in series LS−DRI−DP) at 45 °C (0.05−0.07 w/v % sample concentration). PS standards were obtained from Polymer Laboratories, Amherst, MA, or American Polymer Standards Corporation, Mentor, OH; the Precision LS was calibrated using a narrow PS standard of $M_w = 65\,500$ g/mol.

GPC copolymer molecular weights reported vs PE were determined in 1,2,4-trichlorobenzene (TCB) at 135 °C using either (a) a Waters Associates 150C High-temperature GPC equipped with three Polymer Laboratories mixed bed Type B columns and an internal DRI detector (1.0 mL/min flow rate; typical sample concentration 2 mg/mL), (b) a similar GPC and column suite equipped with in-line triple detection (order: Precision detector 15° LS; Viscotek high-temperature DP; internal DRI) using an 0.5 mL/min flow rate (typical sample concentration 2 mg/mL), or (c) an instrument identical to that in part b except equipped with a Wyatt three-angle mini-DAWN LS detector (typical sample concentration 1−2 mg/mL). PS standards (17 in total) were used for instrument calibration, and a PE calibration curve was then generated via a universal calibration software program[17] using the Mark−Houwink coefficients for PS and PE.

GPC−LS copolymer molecular weights measured at 135 °C in TCB were determined using instruments b and c. Procedures for data analysis and g' calculation are given in the Supporting Information. The Mark−Houwink parameters for PE were used to calculate comparative g' values for polymers having similar composition. Further details for instrument calibration and analysis methodology are given in the Supporting Information.

Copolymer Thermal and Mechanical Analysis. Differential scanning calorimetry (DSC) was carried out on a TA Instruments 2920 calorimeter or a Perkin-Elmer DSC 7 from ≤−110 to 140−160 °C (metathesis copolymers) or from 25 to 200 °C (free-radical copolymers) at 10 °C/min on unannealed samples. Melt transition (T_m) and heat of fusion (ΔH_f) values are derived from second heats; crystallinity (X_c) was calculated by dividing ΔH_f by 293 J/g.[18] Three-point bend and tensile mode DMTA (dynamic mechanical thermal analysis) were carried out using, respectively, a TA Instruments DMA 2980 V1.5B and a Rheometrics Scientific DMTA V fitted with liquid N_2 cooling accessories.

Results and Discussion

Metathesis Copolymerization and Sequence Distribution. As described in the Introduction, metathesis homopolymerization/hydrogenation produces ethylene copolymers having sequence distributions that are fundamentally different from those seen in addition polymerization. Because vinyl addition polymerization assembles chains in two-carbon monomeric units, which can theoretically add in any order or head/tail configuration, methylene run lengths of any size (including $r = 0$) can potentially be present. In contrast, metathesis-based polymerization routes assemble polymer chains in larger, preformed segments with "locked in" sequence distributions around isolated branch points as shown in Schemes 1 and 2.

As depicted in Scheme 3, metathesis copolymerization of comonomers of different sizes and with asymmetrically placed branches produces more "addition-like" alkyl branch-free copolymers containing longer and broader run length distributions. The allowed values of *r* reflect not only the possibilities

Scheme 3. Derivation of Methylene Run Length (*r*) Distributions for Metathesis Polymers Made by the Copolymerization of a Substituted Monomer (R = Functional Group) with a Linear Monomer

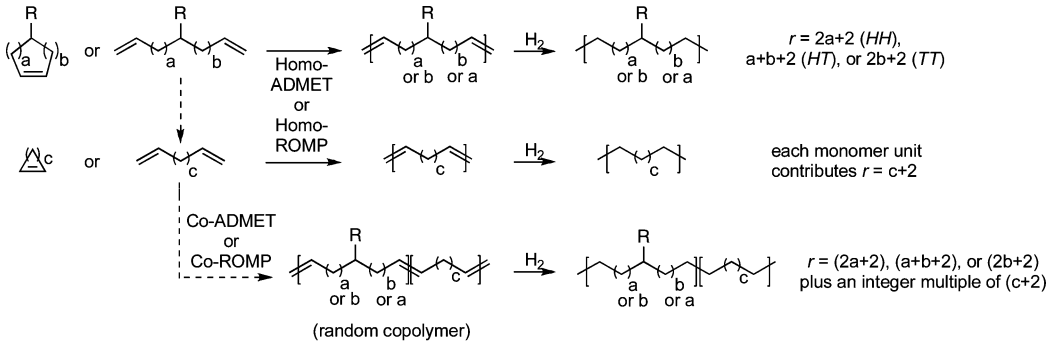

$\therefore$ *r* for random copolymer = [(2a+2) + *x*(c+2)], [(a+b+2) + *x*(c+2)], or [(2b+2) + *x*(c+2)], where *x* = 0,1,2,3,4....

of linear monomers being enchained between substituted monomer units, but also the presence of *pseudo-HH*, *pseudo-HT*, and *pseudo-TT* linkages between each pair of substituted monomer units.

In addition to their alkyl-branch-free nature, these metathesis copolymers exhibit a second advantage over free-radically prepared polyethylenes as models for the study of functional substituent effects in that they contain no polar vinyl comonomer dyads/blocks ($r = 0, 1, 2, 3$). Free-radical ethylene copolymers often have blocky structures, which complicate study of the nature and magnitude of functional group effects: when two substitutents are placed in close proximity, the second occupies an area of the chain that is already functioning as a defect (due to the existence of the first substituent). The dyad-free metathesis copolymers described herein are therefore uniquely advantageous models for understanding the base effects of functional groups on polyethylene properties.

Both ADMET and ROMP strategies were used to prepare the functional polyethylenes via Ru-catalyzed copolymerization of 1,9-decadiene (ADMET) or cyclooctene (ROMP) with appropriate functionalized α,ω-dienes or cyclooctenes, followed by hydrogenation. The polymers were characterized and compared to free-radically prepared, alkyl-branched functional polyethylenes using spectroscopic, light scattering, DSC, and DMTA analysis. ADMET was initially favored for the copolymerizations, given that the chain-addition mechanism of ROMP might be susceptible to reactivity differences between cyclooctene and the functional comonomers. The polycondensation mechanism of ADMET is known to be generally indifferent to polar substituents on α,ω-diene monomers when at least three methylene groups separate the functionalized carbon from the olefin.[19] However, in this particular case, the copolymers prepared via ADMET polycondensation did not have sufficiently high molecular weights for meaningful DMTA analysis (vide infra), and a full suite of model materials was ultimately prepared using ROMP.

ADMET. A series of 11-substituted α,ω-docosadiene comonomers bearing acid, ester, alcohol, and acetate substituents (**1**−**4**, Scheme 4) were synthesized for use in ADMET copolymerization with 1,9-decadiene.[20] In addition to the "randomness" provided by their asymmetry, the comonomers contribute an even number of carbons to the polymer chain, similar to what would occur in true chain-addition copolymerization (each 22-carbon monomer, after loss of its two terminal carbons during ADMET, formally contributes nine ethylene units and one polar vinyl comonomer unit). The carboxylic acid monomer 2-(dec-9-enyl)-tridec-12-enoic acid (**1**) was synthesized by nucleophilic substitution of the dianion of dodec-11-enoic acid onto 11-bromoundecene;[11c,21] the corresponding methyl ester, methyl 2-(dec-9-enyl)-tridec-12-enoate (**2**), was synthesized by reaction of the carboxylate salt of **1** with methyl iodide.[22] The analogous hydroxyl-substituted monomer docosa-1,21-dien-11-ol (**3**) was synthesized by $CeCl_3$-mediated addition of undecen-11-yl magnesium bromide to 10-undecenal[16] (low yields and side products plague the conventional magnesium-mediated Grignard reaction). Alcohol **3** may be acetylated under standard conditions to afford the acetate monomer, acetic acid 1-(dec-9-enyl)-dodec-11-enyl ester (**4**).[11b] All of these monomers may be purified by flash chromatography; **1** and **3** can also be crystallized from cold hexanes.

Scheme 4. Synthesis of Functionalized ADMET Monomers[a]

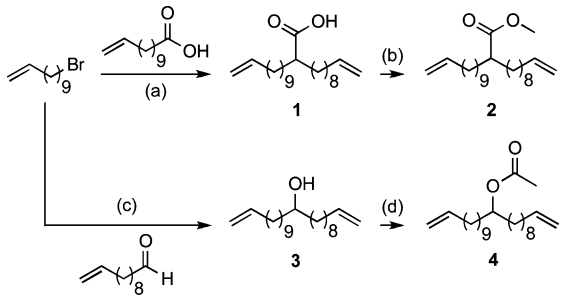

[a] Key: (a) 2 equiv of LDA, THF/DMPU; (b) MeI, K_2CO_3, acetone, Δ; (c) Mg/THF followed by $CeCl_3$; (d) acetic anhydride, DMAP, THF.

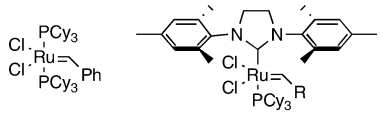

Ru-1 **Ru-2**: R = Ph
Ru-3: R = Me
Ru-4: R = CH=CMe$_2$

Figure 1. Ruthenium metathesis catalysts used for copolymerization.

The "first generation" Grubbs metathesis catalyst $RuCl_2(PCy_3)_2$-CHPh (**Ru-1**, Figure 1) was used for ADMET copolymerizations since it is well-known to promote ADMET of functional monomers,[11a−f] and due to concerns regarding the potential effects of olefin isomerization with more active "second-generation" imidazole-based metathesis catalysts such as $RuCl_2$-(PCy_3)(SIMes)CHPh (**Ru-2**, SIMes = 1,3-dimesitylimidazolidin-2-ylidene, Figure 1).[23] The combination of olefin isomerization in product polyalkenamers at high monomer conversion, and subsequent cross-metathesis between olefins in different polymer chains, would actually provide the beneficial effect of further randomizing copolymer sequence distributions. However, olefin isomerization during ADMET, which is typically conducted under vacuum to increase conversion by removal of ethylene,

Table 1. Polymerization and Hydrogenation Conditions and Characterization Data for Linear Functional Ethylene Copolymers Synthesized via Metathesis

polymer[a]	composition (as mol % polar vinyl)[b]	GPC M_w[c]	GPC M_n[c]	GPC−LS M_w[d]	GPC−LS M_n[d]	T (°C), t	hydr proc
EVOH−1.9-R	1.6 VOH, 0.3 ketene	185 620	80 970			60, 4 d	3
EVOH−1.9-R-2[g]	1.1 VOH, 0.8 ketene	106 340	47 490			60, 6 d	3
EVOH−2.0-R	1.9 VOH, 0.1 ketene	367 280	179 770			25, 3 h	4
EVOH−3.4-R	2.2 VOH, 1.2 ketene	183 990	80 120			60, 1 d	3
EVOH−3.5-R[g]	3.2 VOH, 0.3 ketene	142 070	64 990			60, 6 d	3
EVOH−3.6-R	3.6 VOH	297 040	123 630			25, 2 h	4
EVOH−5.3-R	4.6 VOH, 0.7 ketene	222 390	95 400			60, 1 d	3
EVOH−6.1-R	6.0 VOH, 0.1 ketene	379 460	184 760			25, 4 h	4
EVAC−1.9-R	1.9 VAC	265 330	117 740			60, 2 h	3
EVAC−3.3-R	3.3 VAC	220 230	94 030			60, 20 m	3
EVAC−4.6-R	4.6 VAC	202 940	67 080			60, 20 m	3
EMA−1.9-R	1.9 MA	198 860	91 450			60, 2 h	3
EMA−3.6-R	3.6 MA	202 910	91 500			60, 2 h	3
EMA−5.6-R	5.6 MA	201 980	87 950			60, 2 h	3
ETBA−1.8-R	1.8 tBA	196 990	93 050			60, 2 h	3
ETBA−3.5-R	3.5 tBA	176 600	81 070			60, 20 m	3
ETBA−5.3-R	5.3 tBA	126 720	58 830			60, 2 h	3
EAA−2.6-R	1.5 AA, 0.4 ketene, 0.7 VOH	53 810[f]	12 330[f]			60, 2 h	3
EAA−3.4-R	3.4 AA	38 460[e,f]	20 750[e,f]			60, 3 h	4
EAA−8.3-R	8.3 AA[h]	insol[e]	insol[e]			60, 2 h	3
PE-R	polyethylene	151 370	67 660			60, 15 m	3
EVOH−2.2-A	2.1 VOH, 0.1 ketene	17 060	14 060	17 100	14 000	70, 4 d	1 + 2
EVOH−2.3-A	2.1 VOH, 0.2 ketene	5470	2680	6510	5640	60, 5 d	2
EVOH−4.7-A	3.7 VOH, 1.0 ketene	5350	2530	5530	4950	60, 7 d	1
EVOH−5.1-A	5.0 VOH, 0.1 ketene	9260	2770	6960	5790	60, 3 d	2
EVOH−6.1-A	5.8 VOH, 0.3 ketene	2590	1440			70, 11 d	4
EVAC−2.1-A	1.8 VAC, 0.3 VOH[i]	15 380	5400	14 800	11 800	55, 5 d	1+2
EVAC−6.2-A	6.1 VAC, 0.1 VOH[i]	9280	4450	8810	6100	70, 9 d	2

[a] **R** = ROMP; **A** = ADMET; copolymers with secondary functionalities are named according to their major functional group and the total mol % of functionalities present. [b] Average of ^{1}H and ^{13}C NMR (by ^{13}C NMR for ETBAs); ketene = H$_2$C=C=O. [c] In TCB, 135 °C, vs PE. [d] In TCB, 135 °C, using EVAC parameters. [e] Low solubility. [f] High-MW portion of overlapping bimodal MWD. [g] Prepared using **Ru-4**. [h] By solid-state ^{13}C NMR. [i] Minor hydrolysis of VAC units most likely occurring during workup with acidified workup.

results in both mass loss and compositional alteration through the elimination of volatile higher olefin byproducts.

Bulk vacuum ADMET copolymerizations were carried out with 1,9-decadiene/**3** or /**4** at 55−70 °C for several days to produce polyalkenamers with theoretical compositions of approximately 2, 4, or 6 mol % of the analogous polar vinyl comonomers. Initially, the polymers were hydrogenated by adding chromatographic silica to the diluted polymerization mixture and applying H_2 to form a supported Ru-based hydrogenation catalyst.[11c] This method was complicated by incipient polymer precipitation during separation of the supported catalyst from the hydrogenated polymer solution. More satisfactory results were obtained by isolation of the unsaturated polymer and subsequent hydrogenation with $(Ph_3P)_3RhCl$ (Wilkinson's catalyst) in xylenes.[13] For the EVOH copolymers, both hydrogenation methods resulted in some conversion of alcohol groups to ketones.[24] The most likely mechanism for this interconversion is transfer hydrogenation involving the alcohol group as hydrogen source, which is known to occur with both **Ru-1** and $(Ph_3P)_3RhCl$.[25] The ADMET-derived materials (Table 1) were of relatively low molecular weight (GPC−LS M_w < 20 000 g/mol); compression-molded samples were of insufficient molecular weight for rigorous DMTA analysis. Nevertheless, the materials obtained add the dimension of molecular weight to property studies (it is noted that other functional ADMET materials are now under development with superior properties[11p]).

ROMP. The 5-substituted cyclooctenes **5**−**9** (Scheme 5) were synthesized for use in ROMP copolymerizations with cyclooctene. Cyclooct-4-en-1-ol (**5**) and cyclooct-4-enyl acetate (**6**) were synthesized by the procedure of Hillmyer and Grubbs[6a] and methyl cyclooct-4-enecarboxylate (**7**) was synthesized by the Pd-catalyzed carboxymethylation of 1,5-cyclooctadiene

Scheme 5. Synthesis of Functionalized ROMP Monomers[a]

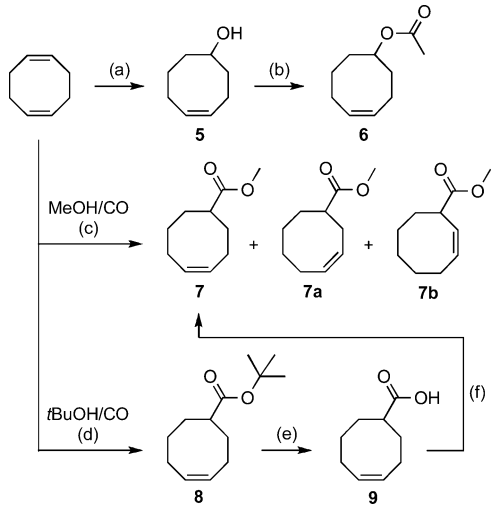

[a] Key: (a) MCPBA/$CHCl_3$ followed by $LiAlH_4$/THF; (b) acetyl chloride, pyridine; (c, d) $PdCl_2$/PPh_3, toluene, Δ; (e) CF_3CO_2H; (f) MeI, K_2CO_3, acetone, Δ.

reported by McLain et al.[6b] The latter reaction leads to a mixture of **7** and its 4- and 3-substituted regioisomers (methyl cyclooct-3-enecarboxylate, **7a**, and methyl cyclooct-2-enecarboxylate, **7b**) in a 28:15:1 ratio. To our delight, we found that substitution of *tert*-butyl alcohol for methanol gives >99% *tert*-butyl cyclooct-4-enecarboxylate (**8**), which can be easily hydrolyzed to cyclooct-4-ene carboxylic acid (**9**).[7b] The isomeric mixture of methyl ester-substituted cyclooctenes **7**/**7a**/**7b** was employed for copolymerization since the mixture actually provides a greater degree of sequence distribution randomness in the copolymer than the single isomer. However, simple base-catalyzed esteri-

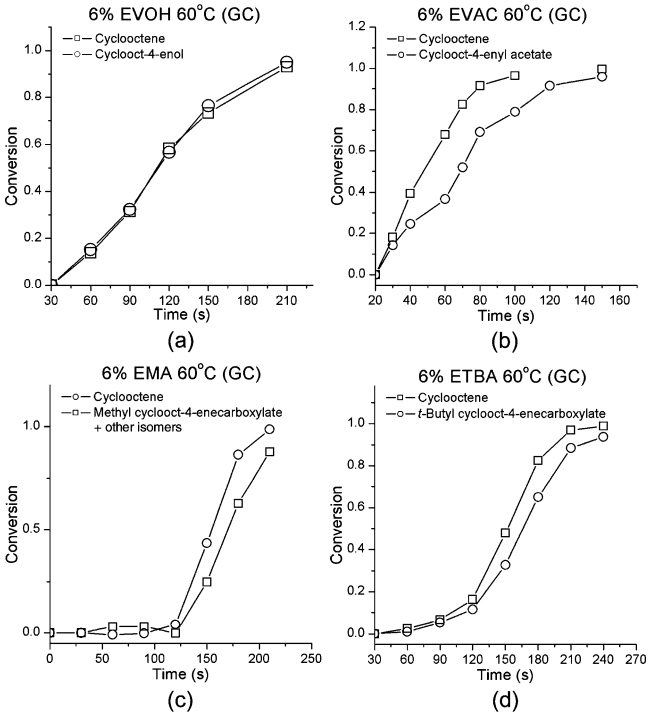

Figure 2. GC kinetic plots of monomer conversions for ROMP copolymerizations at 60 °C: (a) **5**; (b) **6**; (c) **7**/**7a**/**7b**; (d) **8**.

fication[22] of **9** provided >99% isomerically pure **7**, which allowed the identification of the isomer mixture components by ^{1}H NMR and may offer a convenient route into a variety of useful 5-substituted cyclooctene ROMP monomers.

ROMP was conducted on mixtures of cyclooctene and **5**−**9** using "second-generation" imidazole-based Ru catalysts to produce high molecular weight EVAC, EVOH, EMA, EAA, and ETBA copolymers having theoretical 2, 4, and 6 mol % polar vinyl monomer incorporations.[26] Most of the polymerizations were carried out with $RuCl_2(SIMes)(PCy_3)CHCH_3$ (**Ru-3**), an ethylidene complex recently reported by the Wagener group,[14] in order to install rigorously linear alkyl end groups on the polymers during initiation. A few samples were prepared with $RuCl_2(SIMes)(PCy_3)CH{=}CH(CH_3)_2$ (**Ru-4**).[15] Most of the copolymerizations were conducted on an 8−14 g monomer scale at 60 °C in *o*-dichlorobenzene (ODCB), a good solvent for linear polyethylenes (providing convenience for tandem ROMP-hydrogenation), at initial monomer concentrations of 0.4−1.1 M.[27] In contrast to the moderate molecular weight materials obtained with ADMET, ROMP copolymerization gave copolymers with M_ns of 45 000−185 000 g/mol (by GPC vs PE standards) after hydrogenation (Table 1).

The kinetics of the ROMP copolymerizations are important in determining the microstructures of the resultant functional polyethylenes. Equal reactivity of the two comonomers is desired to produce materials that best approximate random copolymers of ethylene and functional vinyl monomers. Kinetics for the 6 mol % polar vinyl EVOH, EVAC, EMA, and ETBA copolymerizations were monitored by GC aliquot analysis (Figure 2). The 60 °C copolymerization kinetics of cyclooctene with alcohol-substituted **5** were found to approach completely random incorporation of the two monomers. However, tracking of the 60 °C copolymerizations involving ester- and acetate-functionalized **6**−**8** indicated that cyclooctene is polymerized at a slightly greater rate than these functional cyclooctenes. Thus, while the copolymerizations were complete within approximately 5 min at 60 °C, they were allowed to proceed for longer periods (typically 2−3 h) in order to promote sequence distribution-randomizing olefin isomerization and cross-metathesis events. Model 4−6 mol % comonomer copolymerizations were also studied at room temperature by ^{1}H NMR and/or GC for **5**, **6**, and **7**/**7a**/**7b**. The relative rates of conversion between the functionalized and unfunctionalized cyclooctene monomers are not altered from those seen at 60 °C although the overall rate of polymerization decreases (total reaction time ≤2 h). Room-temperature ^{1}H NMR kinetics with the **7**/**7a**/**7b** mixture revealed that the 5-substituted isomer **7** is incorporated faster than 4-substituted **7a**, whereas the 3-substituted isomer **7b** is not polymerized.

Most of the ROMP polyalkenamers were hydrogenated by simply applying 400 psig H_2 to the **Ru-3**- or **Ru-4**-containing polymerization solution at 130 °C. A similar procedure has been used by McLain et al. to hydrogenate functional cyclooctene ROMP homopolymers.[6b,28] This in situ Ru-based hydrogenation procedure was satisfactory for the ester- and acetate-containing polymers, but resulted in some conversion of alcohol groups to ketones, as was observed for ADMET EVOHs hydrogenated using **Ru-1**. Ru-catalyzed double bond migration[23] of a polyalkenamer olefin to form an enol followed by tautomerization to the corresponding ketone is a potential mechanism for this transformation (in addition to transfer hydrogenation).[25a] Hydrogenation of one EAA copolymer using **Ru-3** resulted in conversion of some acid groups to secondary alcohols and ketones through an unknown mechanism, presubably via decarbonylation. To circumvent these issues, the remaining EAA polyalkenamers and an additional set of EVOH polyalkenamers were isolated and hydrogenated via diimide reduction using *p*-toluenesulfonhydrazide.[9b] Copolymers hydrogenated using this procedure were largely free of defect functionalities.

Spectral Analysis of Linear Copolymers by NMR and IR. High-temperature ^{1}H and ^{13}C NMR compositional analysis for the model linear functional polyethylenes (reported as the equivalent "mol % ethylene" and "mol % polar vinyl comonomer," Table 1) showed good agreement with compositions expected from monomer feed ratios. ^{13}C NMR EAA analysis was complicated by low polymer solubility and the inability to use $Cr(acac)_3$ relaxation agent (due to ligand exchange with the polymeric acid groups); higher-acid-content copolymers could only be analyzed by ^{1}H NMR or solid-state ^{13}C NMR. The ^{13}C NMR spectra of these rigorously linear copolymers provide non-ambiguous assignments for isolated functional polar vinyl comonomer units (EVE triads) in ethylene/polar vinyl copolymers, without the complexity of short-chain alkyl branching or polar vinyl dyads or triads (EVV or VVV units). The ^{13}C NMR assignments for all of the observed polymer segments are given in Figure 3. Figure 4 shows a spectral comparison for a linear ROMP EVAC and an alkyl-branched free-radical EVAC of similar composition.

The copolymer IR spectra showed two pairs of closely spaced bands at 1473/1463 and 730/720 cm^{-1}, in addition to characteristic bands associated with functional groups. These features are consistent with the orthorhombic phase of polyethylene.[29] EAA IR spectra indicated that the acid groups exist exclusively as hydrogen-bonded dimers in the amorphous phase at room temperature, similar to free-radical EAA copolymers ($\upsilon_{C=O}$ at 1706 cm^{-1} as opposed to 1750 cm^{-1} for free acid groups).[30]

Molecular Weight and Branch Analysis by GPC and GPC—LS. High-temperature GPC analysis using PE standards was used for copolymer molecular weight analysis. Although this technique is complicated by potentially significant, compositionally dependent differences in solution behavior between

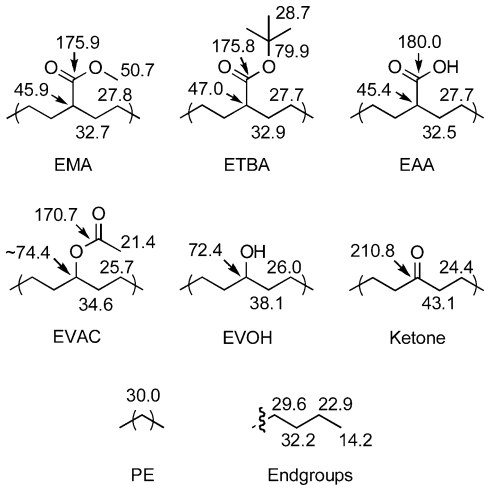

Figure 3. ^{13}C NMR assignments for all observed segments in linear functional polyethylenes (120 °C, ODCB-d_4 (EMA) or TCE-d_2 (all others); the CHO_2CMe peak for EVAC is not resolved from TCE-d_2).

the PE standards and the functionalized materials, it indicated that the ROMP polymers were indeed of high molecular weight ($M_n \geq 45\,000$). The EAA copolymers exhibited apparent molecular weights (vs PE) considerably lower than the other ROMP materials (M_n 12 000−21 000). Given their limited solubility and the fact that no end groups were observed by NMR, it is likely that the EAAs are actually of comparable molecular weight to the other copolymers. GPC−LS analysis of free-radical EVAC, EVOH, and EMA copolymers (using composition-specific input parameters) indicated that GPC underestimates M_n for these "milder" functional materials by a factor of approximately 2−3 (Table SI-2, Supporting Information); it is likely that this effect is more pronounced for the acid-containing materials. The effect of ROMP polymerization temperature on molecular weight is illustrated by the significantly higher M_ns of the three EVOH samples prepared at room temperature (M_n 123 000−185 000 by GPC vs PE) as compared to the samples prepared at 60 °C (M_n 47 000−95 000).

GPC−LS g' calculations were also performed for selected ADMET EVOH and EVAC samples to probe long-chain branch (LCB) content and further confirm the linear nature of the metathesis materials. The g' values for the ADMET copolymers ranged from 0.82 to 1.33[31] and were typically at least twice as high as g' values for free-radical samples of similar composition. For example, an ADMET EVAC containing 2.1 mol % VAC showed a g' value of 1.01, indicating linearity, while an identically composed (2.1 mol % VAC) free-radical copolymer had a g' value of 0.45, indicating significant LCB (Figure SI-3, Supporting Information).

Thermal Analysis by DSC. Substituent Effects on T_m and X_c. The fundamental effects of branches in polyethylenes are generally understood in terms of the Flory exclusion model, whereby branches of sufficient size (two or more non-hydrogen atoms) are excluded from the crystal lattice into the amorphous region.[32] The effect of excluded groups on lowering crystallinity (X_c) and melting point (T_m) is purely colligative in nature, and is independent of branch length or chemical identity at low comonomer contents.[33] Very small functionalities (Cl, OH, = O, Me)[34] are capable of partial inclusion in the polyethylene lattice on an equilibrium basis or as point defects according to the inclusion model of Sanchez and Eby.[35] Groups of intermediate size (such as ethyl) may partially enter crystals to a small extent but more characteristically act as amorphous defects and exert a disordering influence on the lattice.[36]

The thermal properties of free-radical, alkyl-branched, LDPE-like EVOH, EVAC, EMA, and EAA copolymers have been extensively studied.[30a,33b−c,34b,37] Trends for EVAC, EMA, and EAA copolymers are consistent with the exclusion model and similar to those seen for ethylene/α-olefin copolymers; both T_m and X_c decrease rapidly as the amount of pendent functional groups increases.[33c] For example, free-radical EVAC copolymers become completely amorphous at VAC contents of ≥25 mol %.[37c] In contrast, the crystallinity and melting temperatures of free-radical EVOH copolymers are depressed to a lesser extent, due to the smaller size of the OH group and its ability to be partially incorporated into the polyethylene crystal lattice. The behavior of EVOH copolymers therefore more closely resembles that of ethylene/CO and EP copolymers than that of ethylene/α-olefin copolymers.

Sequence distribution effects on the thermal properties of branched and functional polyethylenes are also well-studied.[32,33b,37a,38] For a given substituent content, polymers having a broad distribution of methylene run lengths (and therefore containing longer maximum methylene sequences) typically have higher T_ms than polymers with more evenly distributed substituents. This is not only because their long methylene

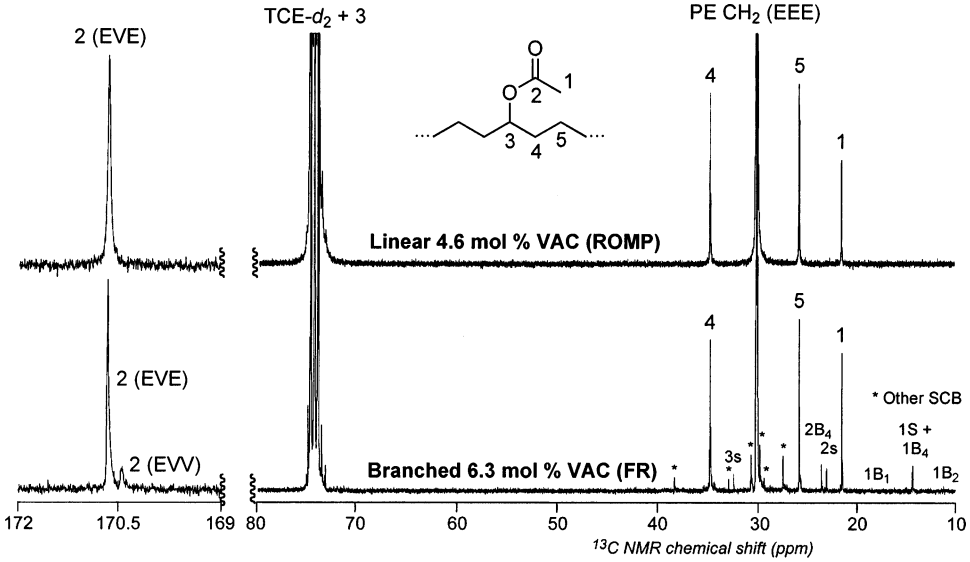

Figure 4. ^{13}C NMR comparison of EVAC copolymers produced by ROMP/hydrogenation and free-radical polymerization.

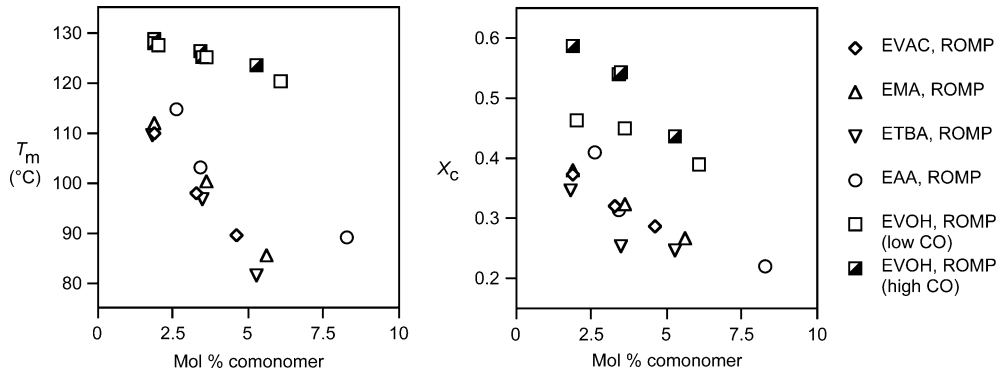

Figure 5. T_m and crystallinity vs mol % comonomer for linear functional polyethylenes prepared by ROMP/hydrogenation (low CO ≤ 0.1 mol % $H_2C{=}C{=}O$ units; high CO ≥ 0.3 mol % $H_2C{=}C{=}O$ units).

Table 2. Thermal and Mechanical Properties of Linear Functional Ethylene Copolymers Synthesized via Metathesis

polymer	T_m(max), °C (X_c)[a]	25 °C storage modulus, MPa (mode)[b]
EVOH−1.9-R	128.8 (0.584)	687 (B)
EVOH−1.9-R-2	127.8 (0.587)	552 (B)
EVOH−2.0-R	127.4 (0.462)	666 (T)
EVOH−3.4-R	126.5 (0.539)	677 (B)
EVOH−3.5-R	125.3 (0.543)	650 (B)
EVOH−3.6-R	125.1 (0.448)	672 (T)
EVOH−5.3-R	123.7 (0.437)	565 (B)
EVOH−6.1-R	120.5 (0.389)	684 (T)
EVAC−1.9-R	109.8 (0.373)	204 (B)[d]
EVAC−3.3-R	97.9 (0.319)[c]	111 (B)
EVAC−4.6-R	89.6 (0.284)[c]	92.1 (B)
EMA−1.9-R	111.8 (0.378)[c]	340 (B)
EMA−3.6-R	100.5 (0.322)[c]	75.8 (B)
EMA−5.6-R	85.4 (0.265)[c]	52.2 (B)[f]
ETBA−1.8-R	109.4 (0.344)[c]	221 (T)
ETBA−3.5-R	96.6 (0.251)[c]	87.9 (T)
ETBA−5.3-R	81.6 (0.246)[c]	49.1 (T)
EAA−2.6-R	114.9 (0.408)	831 (T)
EAA−3.4-R	103.3 (0.312)	463 (T)
EAA−8.3-R	89.0 (0.219)[c]	142 (T)
PE-R	130.8 (0.564)	967 (T)
EVOH−2.2-A	128.5 (0.705)	1418 (B)
EVOH−2.3-A	126.9 (0.830)	
EVOH−4.7-A	123.1 (0.770)	
EVOH−5.1-A	121.8 (0.676)	
EVOH−6.1-A	115.4 (0.659)[c]	
EVAC−2.1-A	117.8 (0.532)	451 (B)
EVAC−6.2-A	73.2 (0.199)[c]	

[a] DSC. [b] DMTA; B = 3-point bend deformation; T = tensile deformation. [c] Broad or with low-temperature shoulder. [d] T = 251 MPa. [e] T = 70.3 MPa.

sequences can crystallize to form relatively large (high-melting) lamellae, but bcause some portion of their substituents are in dyad or block configurations, behaving as one large defect rather than separate defects (lessening the impact per branch). At the other extreme, the content of crystallizable sequences is reduced for copolymers with evenly spaced substituents, and the shorter methylene sequences present generally form smaller lamellae and produce lower T_ms. This effect is strikingly illustrated by the unusually low T_ms (and/or unusually high X_cs and narrow melts due to greater uniformity of crystal size) seen for many "precisely branched" model ADMET polyethylenes.[11b−d,f,i,j,l,n,o,12c,13]

Comparison between Functional Groups for Linear Copolymers. DSC analysis was conducted on the linear ROMP copolymers to measure T_m (maximum) and X_c (Table 2); results are plotted in Figure 5. The ROMP copolymer materials, in contrast to previous functional ADMET models having "precise" sequence distributions, display broad, high-temperature T_ms more characteristic of true random ethylene/polar vinyl copolymers. For all five comonomer types, both T_m and X_c decrease with increasing functional group content. Representative curves

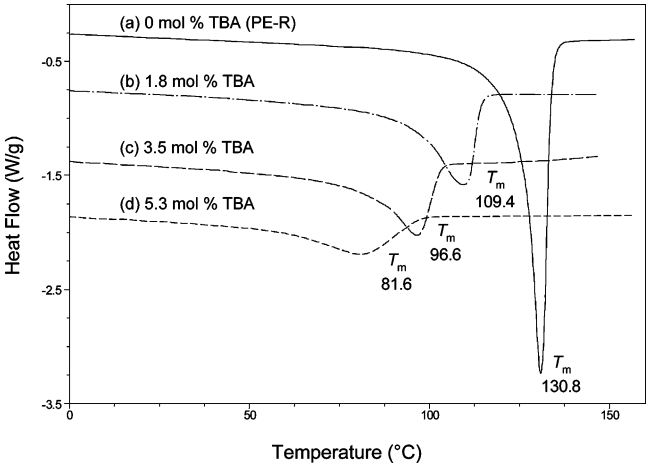

Figure 6. Second heat DSC curves for linear ROMP ETBA copolymers with varying TBA contents.

Table 3. Thermal and Mechanical Properties of Commercial Free-Radical Functional Ethylene Copolymers

polymer	comp (as mol % polar vinyl)[a]	T_m(max), °C (X_c)[b]	25 °C storage modulus, MPa (mode)[c]
EVOH−2.4-FR	2.4 VOH	107.0 (0.470)	361 (B)
EVOH−3.9-FR	3.8 VOH, 0.1 ketene	107.6 (0.487)	182 (B)
EVOH−5.8-FR	5.8 VOH	107.9 (0.405)	209 (B)
EVAC−1.8-FR	1.7 VAC, 0.1 VOH	102.9 (0.313)	82.5 (B)
EVAC−1.9-FR	1.9 VAC	102.5 (0.286)	
EVAC−2.1-FR	2.1 VAC	101.4 (0.315)	78.1 (B)
EVAC−3.0-FR	3.0 VAC	96.2 (0.278)	56.7 (B)
EVAC−3.0-FR-2	3.0 VAC	98.8 (0.262)	64.6 (B)
EVAC−4.0-FR	4.0 VAC	92.2 (0.227)	32.5 (B)
EVAC−5.3-FR	5.3 VAC	88.6 (0.163)	28.1 (B)
EVAC−6.3-FR	6.3 VAC	84.9 (0.152)	26.6 (B)
EMA−2.0-FR	2.0 MA	100.8 (0.311)	
EMA−2.2-FR	2.2 MA	101.1 (0.287)	140 (B)
EMA−3.3-FR	3.3 MA	99.7 (0.263)	
EMA−4.9-FR	4.9 MA	88.3 (0.184)	22.2 (B)
EMA−5.7-MA	5.7 MA	86.4 (0.165)	26.6 (B)
EMA−7.8-FR	7.8 MA	75.1 (0.078)	14.9 (B)
EMA−11.4-FR	11.4 MA	64.6 (0.035)	12.0 (B)
EAA−1.9-FR	1.9 AA	97.5 (0.284)	344 (T)
EAA−2.4-FR	2.4 AA	102.5 (0.312)	
EAA−3.3-FR	3.3 AA	95.1 (0.195)[d]	196 (T)
EAA−3.3-FR-2	3.3 AA	98.3 (0.255)	193 (T)[e]
EAA−3.7-FR	3.7 AA	96.0 (0.234)	
EAA−3.8-FR	3.8 AA	95.3 (0.231)	
EAA−5.5-FR	5.5 AA	83.4 (0.099)	38.8 (T)
EAA−6.4-FR	6.4 AA	89.2 (0.141)	

[a] Average of ^1H and ^{13}C NMR. [b] DSC; all T_ms except for EVOHs were broad or exhibited a low-temperature shoulder. [c] DMTA; B = 3-point bend deformation; T = tensile deformation. [d] Two maxima, 92.0 and 98.1 °C. [e] B = 158 MPa.

for ETBA copolymers are shown in Figure 6. As predicted by the Flory exclusion model and literature data for other branched polyethylenes, the identity of the functional groups in the EVAC,

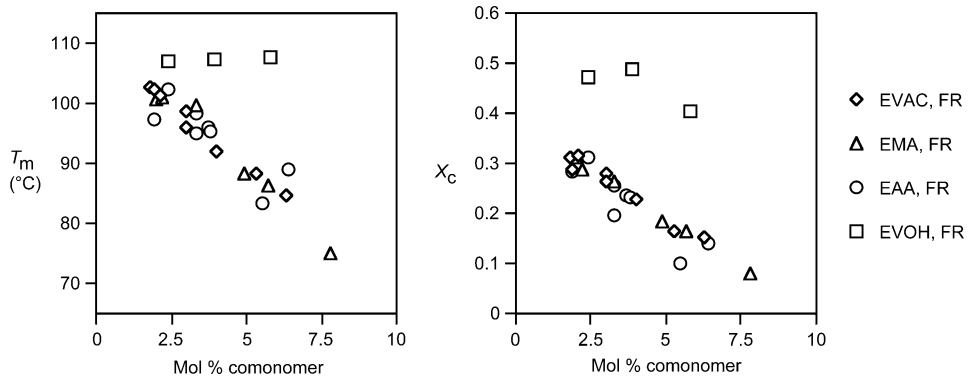

Figure 7. T_m and crystallinity vs mol % comonomer for alkyl-branched free-radical functional polyethylenes.

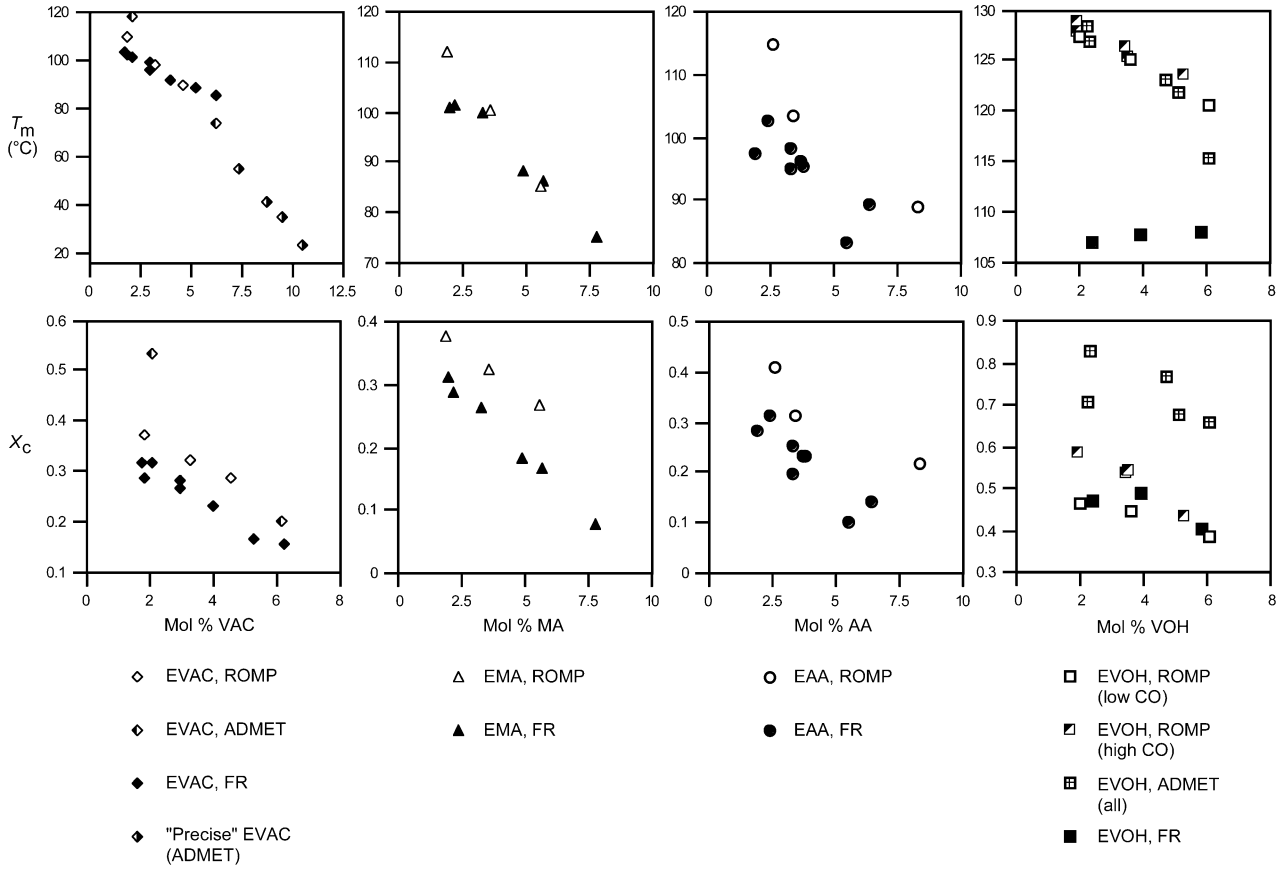

Figure 8. T_m (top) and crystallinity (bottom) comparison for linear (methathesis/hydrogenation) vs alkyl-branched (free-radical) functional polyethylenes (low CO ≤ 0.1 mol % $H_2C{=}C{=}O$ units; high CO ≥ 0.3 mol % $H_2C{=}C{=}O$ units). Comparative "precisely branched" homo-ADMET EVAC data taken from ref 11b.

EMA, and ETBA copolymers is irrelevant. T_m and X_c for these three series vary only with comonomer content. Compositional uncertainties for the ROMP EAA copolymers complicate a determination of whether the acid group behaves similarly: two of the EAA copolymers (**EAA−2.6-R** and **EAA−8.3-R**) exhibited T_ms and X_cs higher than those for the ester/acetate-substituted copolymers. This may potentially be explained by the presence of secondary alcohol groups and ketones in **EAA−2.6-R** and uncertainty from use of a different compositional analysis method (solid-state ^{13}C NMR) for **EAA−8.3-R**. No significant T_m and X_c differences are observed between acid- and ester/acetate-substituted free-radically prepared copolymers (vide infra).

Consistent with partial substituent inclusion into the crystalline phase,[33b] the melting temperatures of the EVOH metathesis copolymers were much higher (and narrower) than those for the acid- and ester/acetate-functionalized copolymers, and showed a gentler depression in T_m per comonomer unit. Partial replacement of the OH substituents with ketones ("high CO" samples, Figure 5) did not affect T_m but increased X_c and the sensitivity of X_c to composition. It is possible that the lower X_cs seen for the CO-free EVOHs as compared to the "high CO" samples are a reflection of their higher molecular weights.[33e,39]

Effects of Alkyl Branching and Molecular Weight. A suite of low-polar-content free-radical EVAC, EMA, and EAA copolymers, containing 10−43 short-chain alkyl branches per 1000 total carbons (Table SI-2, Supporting Information), was studied for comparison to the linear ROMP materials. Comparative alkyl-branched EVOH copolymers were prepared by hydrolysis of branched EVACs. DSC T_m and X_c data for the free-radical materials (Table 3) are plotted in Figure 7. DSC curve shapes and general trends parallel those seen for the linear

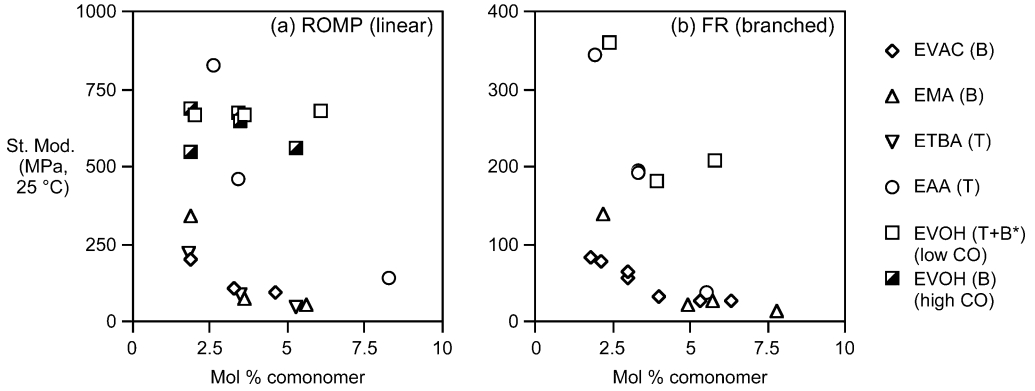

Figure 9. Room-temperature storage moduli for (a) linear (ROMP/hydrogenation) and (b) alkyl-branched (free-radical) functional polyethylenes (low CO = ≤0.1 mol % $H_2C{=}C{=}O$ units; high CO = ≥0.3 mol % $H_2C{=}C{=}O$ units). B = three-point bend mode; T = tensile mode (*ROMP = T, FR = B).

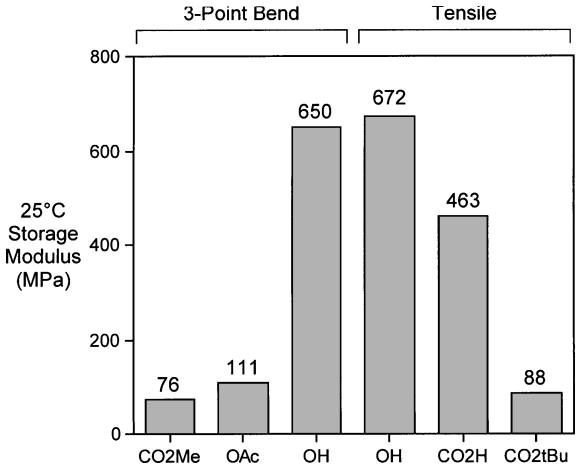

Figure 10. Functional group effects on modulus for linear functional polyethylenes having similar composition (left to right): **EMA−3.6-R**, **EVAC−3.3-R**, **EVOH−3.5-R** (0.3 mol % $H_2C{=}C{=}O$), **EVOH−3.6-R**, **EAA−3.4-R**, and **ETBA−3.5-R**.

copolymers: the branched ester/acetate-substituted materials exhibit colinear depressions in T_m and X_c with no functionality-specific effects, while the branched EVOHs show comparatively higher and narrower T_ms, greater X_cs, and a reduced sensitivity of both to composition. Overall, the branched EAA materials do not show behavioral differences from the ester/acetate-substituted copolymers.

T_m and X_c comparisons between each set of linear and alkyl-branched copolymers are given in Figure 8. The linear ester- and acetate-substituted ROMP copolymers show higher T_ms than the branched copolymers at the lowest comonomer contents (below ca. 4 mol %), although the differences are small (Figure 8, top). The linear and branched T_m vs composition curves converge at ca. 4−7 mol % comonomer. Compositional uncertainties for samples **EAA−2.6-R** and **EAA−8.3-R** obscure trends for the acid-substituted copolymers, although the data is suggestive of a similar relationship. In contrast, the linear ROMP EVOHs showed higher T_ms than the alkyl-branched copolymers at all compositions, consistent with partial OH inclusion into the crystal lattice and exclusion of the free-radical copolymer alkyl branches. The ADMET EVAC and EVOH materials (also plotted in Figure 8) had T_ms similar to those for the higher-M_n ROMP materials.

This data point suggests that at comonomer contents of greater than ∼7 mol %, linear functional copolymers with larger "excluded" substituents will have equal or lower T_ms than alkyl-branched materials, despite the fact that the linear polymers contain fewer overall chain punctuations. Linear materials with >7 mol % randomly distributed polar comonomer were not available to probe this regime. However, assuming an extension of the linear relationship between alkyl-branched copolymer T_m and mol % VAC into this compositional range as a lower boundary,[33c,40] the T_ms for "precisely" branched model ADMET EVACs having 7.4−10.5 mol % VAC[11b] do indeed fall below those predicted for alkyl-branched samples (Figure 8, top left). On the basis of the "leveling" effect of alkyl branches and the greater run length-shortening effect of more evenly distributed substituents, "precisely" functionalized substituents would be expected to show the greatest per-unit lowering effect on T_m, with functional groups on alkyl-branched copolymers showing the weakest effect, and "random" linear materials intermediate between the two.

The linear copolymers with "excluded" acid and ester/acetate substituents showed higher X_cs than the branched copolymers at all compositions studied (Figure 8, bottom). Interestingly, while the "high CO" ROMP EVOH materials had, on average, higher X_cs than the alkyl-branched EVOHs, the CO-free ROMP EVOHs were not demonstrably more crystalline than the branched EVOHs despite their linearity. Again, this may reflect the higher molecular weights of the three CO-free EVOH samples; crystallinities for the all of the low-M_n ADMET materials (both high- and low-CO EVOH and EVAC) were decidedly higher than those for analogous ROMP samples.

Thermomechanical Analysis by DMTA. While T_m and X_c are functions of a material's crystalline fraction, the storage modulus of a semicrystalline polymer reflects both its crystallinity and the cross-link density of its amorphous phase. Moduli measurements are therefore potentially more sensitive to chemical differences between functional substituents (even those excluded from the crystalline phase). Relationships between composition and mechanical properties for alkyl-branched free-radical EVAC and EVOH copolymers have been studied by Nielsen[37d] and Salyer and Kenyon.[37c] For EVACs, shear modulus, Clash−Berg modulus, and tensile strength were found to decrease with increasing VAC content. However, since mechanical properties are particularly sensitive to branch identity and content, trends observed for highly branched functional polyethylenes may not be predictive for linear materials.

Temperature-dependent DMTA modulus data were collected on compression-molded linear and free-radical functional copolymer samples using either tensile or three-point bend deformation (Tables 2 and 3).[41] Plots of 25 °C storage moduli vs comonomer content are shown in Figure 9. Moduli ranged between 10 and 700 MPa, as compared to 967 MPa for a perfectly linear unfunctionalized polyethylene prepared by ROMP/hydrogenation (the low-M_n ADMET materials showed

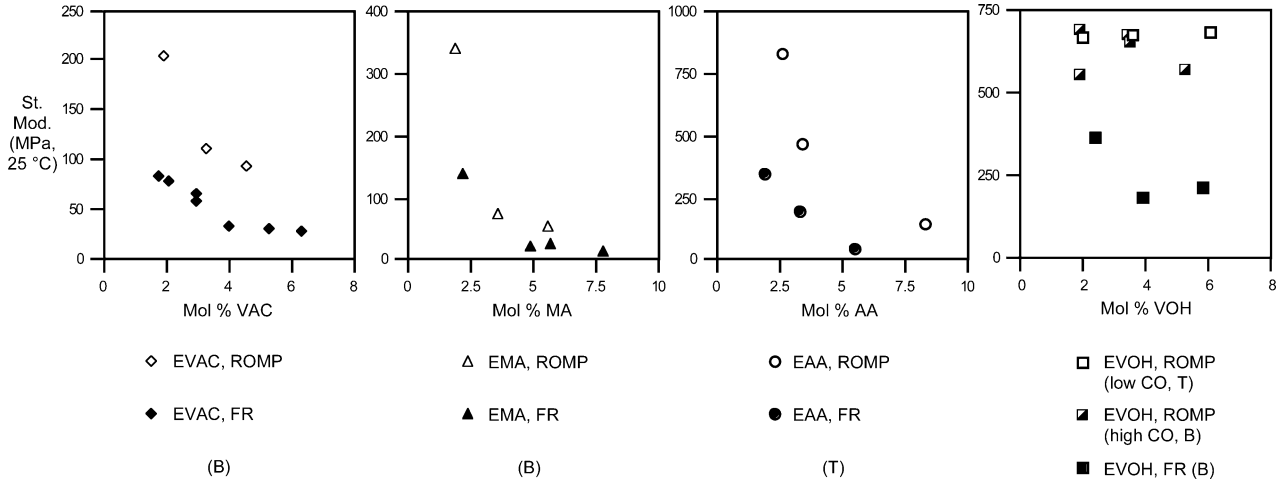

Figure 11. Storage modulus comparison for linear (ROMP/hydrogenation) vs alkyl-branched (free-radical) functional polyethylenes (low CO ≤ 0.1 mol % $H_2C{=}C{=}O$ units; high CO ≥ 0.3 mol % $H_2C{=}C{=}O$ units). B = three-point bend mode; T = tensile mode.

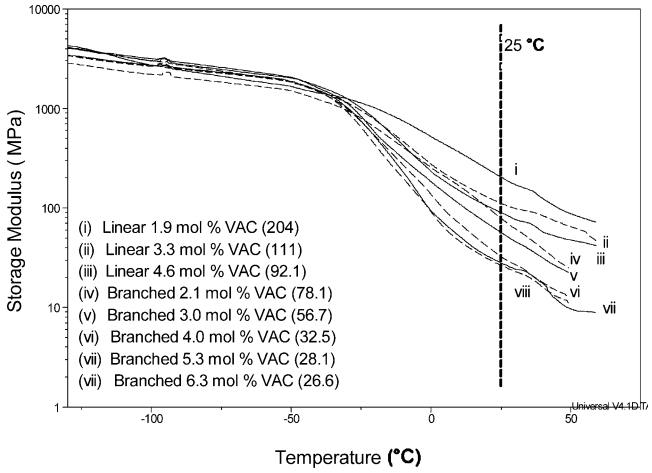

Figure 12. Three-point bend mode DMTA curves for linear and branched EMA copolymers (25 °C modulus values in parentheses).

anomalously high moduli of 450−1420 MPa, 1.5−2.5 times greater than ROMP materials of similar composition, and are not included in Figure 9). For both linear and alkyl-branched ester/acetate-substituted copolymers, 25 °C storage modulus decreases with increasing functional group content. Modulus values are not sensitive to the identity of the functional substituent except possibly at the very lowest comonomer contents, where moduli for EMAs were higher than for EVACs and ETBAs. This general trend is consistent with a colligative crystallinity-depressing effect involving excluded, weakly interacting substituent groups. Modulus also decreases with increasing acid content for the EAA copolymers (reflecting a dominating factor of loss of crystallinity), but values are higher than for the analogous ester/acetate-substituted copolymers, presumably as a result of amorphous-phase hydrogen bonding between acid groups. Overall, the OH-substituted copolymers had the highest moduli, consistent with the alcohol group's ability to both enter the crystal and potentially participate in amorphous cross-links (vide infra). This effect was most pronounced for the linear EVOH copolymers, which, in contrast to the alkyl-branched materials, showed no apparent sensitivity to composition.[42] A summary comparison of functional group effects for linear copolymers having ca. 3.5 mol % polar comononer is given in Figure 10.

Storage modulus comparisons for each linear vs alkyl-branched copolymer set are given in Figure 11; representative DMTA curves for EVAC materials are shown in Figure 12. The ester/acetate- and acid-substituted copolymers showed relationships very similar to those exhibited for T_m: the relatively higher moduli of the linear materials at low comonomer content appeared to trend toward convergence with those for alkyl-branched materials at ca. 5−6 mol % comonomer. By contrast (and also analogous to T_m trends), moduli for the linear EVOH copolymers were higher than those for the alkyl-branched copolymers at all studied compositions. The unusual insensitivity of modulus to VOH content for the linear EVOH polymers is interesting. The OH substituents in alkyl-branched EVOH materials are known to associate via hydrogen bonding.[37c,43] It is likely that removing the alkyl branches in EVOHs allows for more efficient hydrogen bonding interactions between OH groups in the amorphous phase, and, unlike for the excluded acid groups in EAAs, possibly also in the crystalline phase. This may explain the superior T_ms, crystallinities, and storage moduli observed for these materials.

Conclusions

Alkyl-branch-free polyethylenes were synthesized by ruthenium-catalyzed olefin metathesis copolymerization followed by polymer hydrogenation and were shown to be structurally equivalent to copolymers of ethylene and <10 mol % of polar vinyl monomers by NMR characterization. The ROMP copolymerizations of cyclooctene with ester- and alcohol-functionalized cyclooctenes were shown to proceed in a primarily random fashion to give polymers with homogeneous distributions of functional groups along the backbone. These polymers differ from previous metathesis-derived linear PE analogues in that they do not have precise sequence distributions, and therefore serve as superior models for chain-addition functional PEs. The methyl ester-, *tert*-butyl ester-, and acetate-substituted polymers display a rapid decrease in melting temperature, heat of fusion, and storage modulus with increasing comonomer content. The thermal properties of these three copolymers are similar irrespective of the identity of the functional group or the molecular weight in the range studied, consistent with these groups being equally excluded from the crystal lattice. The alcohol-substituted polymers, however, show comparatively higher T_ms and storage moduli, and much less drastic decreases in melting temperature and heat of fusion with increasing comonomer content compared to the ester-substituted polymers. Acid-substituted polymers appeared to behave similarly to ester- and acetate-substituted polymers in terms of T_m and crystallinity, but showed room-temperature storage moduli intermediate

between the ester- and acetate-containing polymers and the alcohol-containing polymers.

The main conclusion from these experiments is that the primary behavior of alkyl-branch-free functionalized polyethylenes is consistent with the large body of previous work involving the effects of functional substituents on polyethylenes, which have been carried out utilizing free-radical (alkyl-branch-containing) materials.

Acknowledgment. We thank Boming Liang, Joseph Olkusz, Mark Genowitz, Richard Flynn, Jim Balogh, Thomas Brown, and Henry Dong for assistance with NMR, GPC, DSC, and DMTA analysis and sample molding; Dr. Jonathan Schulze (ExxonMobil Chemical Co.) for tensile-mode DMTA data; Dr. Louise Wheeler for GPC−LS and g' analysis; and Wendell Bobb for preparation of alkyl-branched EVOH copolymers.

Supporting Information Available: Text giving synthetic procedures for all copolymer samples, alkyl-branched EVOH copolymers, and monomers **1**−**4** and **7**−**9**, ROMP copolymerization kinetics procedures and figures showing room-temperature kinetics plots, text giving characterization data (NMR, IR, GPC/GPC−LS, DSC, DMTA) for free-radical copolymers and selected polyalkenamers, procedures for GPC−LS triple detector calibration and d*n*/d*c* calculation, copolymer NMR compositional and branch analysis, DMTA analysis and preparation of sample bars, tables of copolymer DSC crystallization temperatures (T_c) and X_cs, and a figure giving graphical g' comparison between linear and branched EVAC copolymers. This material is available free of charge via the Internet at http://pubs.acs.org.

References and Notes

(1) Boffa, L. S.; Novak, B. M. *Chem. Rev.* **2000**, *100*, 1479−1494.

(2) Doak, K. W. In *Encyclopedia of Polymer Science & Engineering*, 2nd ed.; Mark, H. F., Bikales, N. M., Overberger, C. G., Menges, G., Kroschwitz, J. I., Eds.; John Wiley & Sons: New York, 1986; Vol. 6, pp 386−429.

(3) Klimesch, R.; Littmann, D.; Mähling, F.-O. Polyethylene: High Pressure. In *Encyclopedia of Materials: Science and Technology*; Buschow, K. H. J., Cahn, R. W., Flemings, M. C., Ilschner, B., Kramer, E. J., Mahajan, S., Eds.; Elsevier Science: New York, 2004; pp 7181−7184.

(4) Enderle, H. F. Polyethylene: High Density. In *Encyclopedia of Materials: Science and Technology*; Buschow, K. H. J., Cahn, R. W., Flemings, M. C., Ilschner, B., Kramer, E. J., Mahajan, S., Eds.; Elsevier Science: New York, 2004; pp 7172−7180.

(5) (a) Johnson, L. K.; Mecking, S.; Brookhart, M. *J. Am. Chem. Soc.* **1996**, *118*, 267−268. (b) Mecking, S.; Johnson, L. K.; Wang, L.; Brookhart, M. *J. Am. Chem. Soc.* **1998**, *120*, 888−889. (c) Johnson, L.; Bennett, A.; Dobbs, K.; Hauptman, E.; Ionkin, A.; Ittel, S.; McCord, E.; McLain, S.; Radzewich, C.; Yin, Z.; Wang, L.; Wang, Y.; Brookhart, M. *Polym. Mater. Sci. Eng.* **2002**, *86*, 319. (d) Wang, C.; Friedrich, S.; Younkin, T. R.; Li, R. T.; Grubbs, R. H; Bansleben, D. A.; Day, M. W. *Organometallics* **1998**, *17*, 3149−3151. (e) Younkin, T. R.; Connor, E. F.; Henderson, J. I.; Friedrich, S. K.; Grubbs, R. H.; Bansleben, D. A. *Science* **2000**, *287*, 460−462. (f) Connor, E. F.; Younkin, T. R.; Henderson, J. I.; Hwang, S.; Grubbs, R. H.; Roberts, W. P.; Litzau, J. I. *J. Polym. Sci., Part A: Polym. Chem.* **2002**, *40*, 2842−2854. (g) Drent, E.; van Dijk, R.; van Ginkel, R.; van Oort, B.; Pugh, R. I. *Chem. Commun. (Cambridge)* **2002**, 744−745. (h) Kochi, T.; Yoshimura, K.; Nozaki, K. *J. Chem. Soc., Dalton Trans.* **2006**, 25−27. (i) Stibrany, R. T.; Schulz, D. N.; Kacker, S.; Patil, A. O.; Baugh, L. S.; Rucker, S. P.; Zushma, S.; Berluche, E.; Sissano, J. A. *Macromolecules* **2003**, *36*, 8584−8586. (j) Baugh, L. S.; Sissano, J. A.; Kacker, S.; Berluche, E.; Stibrany, R. T.; Schulz, D. N.; Rucker, S. P. *J. Polym. Sci., Part A: Polym. Chem.* **2006**, *44*, 1817−1840.

(6) (a) Hillmyer, M. A.; Laredo, W. R.; Grubbs, R. H. *Macromolecules* **1995**, *28*, 6311−6316. (b) McLain, S. J.; McCord, E. F.; Arthur, S. D.; Hauptman, E.; Feldman, J.; Nugent, W. A. *Polym. Mater. Sci. Eng.* **1997**, *76*, 246−247. (c) Bansleben, D. A.; Huynh-Tran, T.-C.; Blanski, R. L.; Hughes, P. A.; Roberts, W. P.; Grubbs, R. H.; Hatfield, G. R. (Cryovac). PCT Int. Pat. Appl. WO00/18579, Apr 6, 2000; U.S. Patent 6,203,293, March 20, 2001. (d) Cho, S. Y.; Cho, U. H. (Korea, Adv. Inst. Sci. Tech.). Korean Pat. Appl. KR2001036073A, May 7, 2001; Korean Patent KR349626, August 22, 2002. (e) Stephens, C. H.; Yang, H.; Islam, M.; Rowan, S. J.; Hiltner, A.; Baer, E. *Annu. Tech. Conf.-Soc. Plast. Eng.* **2002**, *60th (Vol. 2)*, 1854−1858. (f) Yang, H.; Islam, M.; Budde, C.; Rowan, S. J. *J. Polym. Sci., Part A: Polym. Chem.* **2003**, *41*, 2107−2116. (g) Stephens, C. H.; Yang, H.; Islam, M.; Chum, S. P.; Rowan, S. J.; Hiltner, A.; Baer, E. *J. Polym. Sci., Part B: Polym. Phys.* **2003**, *41*, 2062−2070.

(7) Noels and Democeau et al. have also homopolymerized a wide variety of functionalized cyclooctenes using ROMP; however, these materials were not hydrogenated: (a) Stumpf, A. W.; Saive, E.; Demonceau, A.; Noels, A. F. *J. Chem. Soc., Chem. Commun.* **1995**, 1127−1128. (b) Demonceau, A.; Stumpf, A. W.; Saive, E.; Noels, A. F. *Macromolecules* **1997**, *30*, 3127−3136. (c) Noels, A. F.; Demonceau, A. In *Metathesis Polymerization of Olefins and Polymerization of Alkynes*; Imamoglu, Y., Ed.; NATO ASI Series C., Math. Phys. Sci. 506. Kluwer: Dordrecht, The Netherlands, 1998; pp 29−46.

(8) Cho and Cho have similarly used homopolymerization/hydrogenation of cyclododeca-4,6-dienyl acetate to prepare polyethylenes containing 16.6 mol % of vinyl acetate or vinyl alcohol.[6d]

(9) (a) Bansleben, D. A.; Huynh-Tran, T.-C. T.; Blanski, R. L.; Hughes, P. A.; Roberts, W. P.; Grubbs, R. H.; Hatfield, G. R. (Cryovac). PCT Int. Pat. Appl. WO99/50331, October 7, 1999; U.S. Patent 6,153,-714, Nov 28, 2000; U.S. Patent 6,506,860, Jan 14, 2003. (b) Scherman, O. A.; Kim, H. M.; Grubbs, R. H. *Macromolecules* **2002**, *35*, 5366−5371. (c) Scherman, O. A.; Walker, R.; Grubbs, R. H. *Macromolecules* **2005**, *38*, 9009−9014. (d) Jordan, J. P.; Scherman, O. A.; Grubbs, R. H. *Polym. Prepr. (Am. Chem. Soc., Div. Polym. Chem.)* **2003**, *44* (1), 841−842.

(10) (a) Ramakrishnan, S.; Chung, T. C. *Macromolecules* **1990**, *23*, 4519−4524. (b) Chung, T. C. *Polymer* **1991**, *32*, 1336−1339. (c) Weaver, J. D.; Harris, W. J.; Hill, S. E.; Cheung, Y. W. (Dow). PCT Int. Pat. Appl. WO03/078499, Sept 25, 2003.

(11) (a) Watson, M. D.; Wagener, K. B. *Macromolecules* **2000**, *33*, 3196−3201. (b) Watson, M. D.; Wagener, K. B. *Macromolecules* **2000**, *33*, 5411−5417. (c) Watson, M. D.; Wagener, K. B. *Macromolecules* **2000**, *33*, 8963−8970. (d) Boz, E.; Wagener, K. B.; Ghosal, A.; Fu, R.; Alamo, R. G. *Macromolecules* **2006**, *39*, 4437−4447. (e) Boz, E.; Nemeth, A. J.; Alamo, R. G.; Wagener, K. B. *Adv. Synth. Catal.* **2007**, *349*, 137−141. (f) Schwendeman, J. E.; Wagener, K. B. *Macromolecules* **2004**, *37*, 4031−4037. (g) Baughman, T. W.; van der Aa, E.; Lehman, S. E.; Wagener, K. B. *Macromolecules* **2005**, *38*, 2550−2551. (h) Baughman, T. W.; van der Aa, E.; Wagener, K. B. *Macromolecules* **2006**, *39*, 7015−7021. (i) Wagener, K. B.; Valenti, D. J.; Hahn, S. F. *Macromolecules* **1997**, *30*, 6688−6690. (j) Smith, J. A.; Brzezinska, K. R.; Valenti, D. J.; Wagener, K. B. *Macromolecules* **2000**, *33*, 3781−3794. (k) Schwendeman, J. E.; Wagener, K. B. *Macromol. Chem. Phys.* **2005**, *206*, 1461−1471. (l) Sworen, J. C.; Smith, J. A.; Berg, J. M.; Wagener, K. B. *J. Am. Chem. Soc.* **2004**, *126*, 11238−11246. (m) Sworen, J. C.; Berg, J. M.; Wagener, K. B. *Polym. Prepr. (Am. Chem. Soc., Div. Polym. Chem.)* **2004**, *45* (1), 961−962. (n) Schwendeman, J. E.; Watson, M. D.; Smith, J. A.; Brzezinska, K. R.; Wagener, K. B. In *Ring Opening Metathesis Polymerization and Related Chemistry*; Khosravi, E., Szymanska-Buzar, T., Eds.; NATO Sci. Ser. II, Math. Phys. Chem. 56. Kluwer: Dordrecht, The Netherlands, 2002; pp 307−319. (o) Baughman, T. W.; Wagener, K. B. *Adv. Polym. Sci.* **2005**, *176*, 1−42. (p) Baughman, T. W.; Chan, C.; Opper, K. L.; Wagener, K. B.; Winey, K. I. *Polym. Mat. Sci. Eng.* **2006**, *95*, 140.

(12) (a) Baughman, T. W.; Sworen, J. C.; Wagener, K. B. *Macromolecules* **2006**, *39*, 5028−5036. (b) Lieser, G.; Wegner, G.; Smith, J. A.; Wagener, K. B. *Colloid Polym. Sci.* **2004**, *282*, 773−781. (c) Qiu, W.; Sworen, J. C.; Pyda, M.; Nowak-Pyda, E.; Habenschuss, A.; Wagener, K. B.; Wunderlich, B. *Macromolecules* **2006**, *39*, 204−217.

(13) Sworen, J. C.; Smith, J. A.; Wagener, K. B.; Baugh, L. S.; Rucker, S. P. *J. Am. Chem. Soc.* **2003**, *125*, 2228−2240.

(14) Lehman, S. E., Jr.; Wagener, K. B. *Organometallics* **2005**, *24*, 1477−1482.

(15) Chatterjee, A. K.; Morgan, J. P.; Scholl, M.; Grubbs, R. H. *J. Am. Chem. Soc.* **2000**, *122*, 3783−3784.

(16) Imamoto, T.; Takiyama, N.; Nakamura, K.; Hatajima, T.; Kamiya, Y. *J. Am. Chem. Soc.* **1989**, *111*, 4392−4398.

(17) Sun, T.; Brant, P.; Chance, R. R.; Graessley, W. W. *Macromolecules* **2001**, *34*, 6812−6820.

(18) Wunderlich, B. *Macromolecular Physics, Vol. 1: Crystal Structure, Morphology, Defects*; Academic Press: New York, 1973; pp 401−407.

(19) Wagener, K. B.; Brzezinska, K. *Macromolecules* **1991**, *24*, 5273−5277.

(20) Using the depiction in Scheme 3 ($a = 8$, $b = 9$, $c = 6$), run lengths present in the product hydrogenated copolymers are $r = 18 + 8x$, $19 + 8x$, and $20 + 8x$ (where $x =$ integer ≥ 0); i.e. $r = 18$, 19, 20, 26, 27, 28, 34, 35, 36, etc.

(21) The literature involving this reaction calls for the use of the carcinogenic solvent hexamethylphosphoramide (HMPA). Numerous attempts were made to substitute the more innocuous solvent 1,3-dimethyl-3,4,5,6-tetrahydro-2(*1H*)-pyrimidinone (DMPU). Although the reaction does proceed using DMPU, the superior results obtained with HMPA could not be attained.
(22) Moore, G. G.; Foglia, T. A.; McGahan, T. J. *J. Org. Chem.* **1979**, *44*, 2425−2429.
(23) (a) Lehman, S. E., Jr.; Schwendeman, J. E.; O'Donnell, P. M.; Wagener, K. B. *Inorg. Chim. Acta* **2003**, *345*, 190−198. (b) Hong, S. H.; Day, M. W.; Grubbs, R. H. *J. Am. Chem. Soc.* **2004**, *126*, 7414−7415. (c) Hong, S. H.; Sanders, D. P.; Lee, C. W.; Grubbs, R. H. *J. Am. Chem. Soc.* **2005**, *127*, 17160−17161.
(24) To maintain the "polar vinyl" basis used for polymer composition, these groups were quantified as theoretical ketene ($H_2C{=}C{=}O$) monomer units.
(25) (a) Louie, J.; Bielawski, C. W.; Grubbs, R. H. *J. Am. Chem. Soc.* **2001**, *123*, 11312−11313. (b) Nishiguchi, T.; Tachi, K.; Fukuzumi, K. *J. Org. Chem.* **1975**, *40*, 237−240.
(26) Using the depiction in Scheme 3 ($a = 2$, $b = 3$, $c = 6$), run lengths present in the product hydrogenated copolymers are $r = 6 + 8x$, $7 + 8x$, and $8 + 8x$; i.e. $r = 6$, 7, 8, 14, 15, 16, 22, 23, 24, 30, 31, 32, etc.
(27) Monomer concentration is an important parameter for use in suppressing formation of cyclic oligomers during ROMP. Ideally, copolymerizations would be conducted in bulk to best favor the formation of linear polymer. However, the high solution viscosities seen for polymerizations carried out at $[\text{monomer}]_o > 0.9$ M precluded facile handling and transfer to hydrogenation vessels.
(28) Other tandem Ru-based polyalkenamer hydrogenations are known: (a) Drouin, S. D.; Yap, G. P. A.; Fogg, D. E. *Inorg. Chem.* **2000**, *39*, 5412−5414. (b) Drouin, S. D.; Zamanian, F.; Fogg, D. E. *Organometallics* **2001**, *20*, 5495−5497. (c) Fogg, D. E.; Amoroso, D.; Drouin, S. D.; Snelgrove, J.; Zamanian, F. *J. Mol. Catal. A: Chem.* **2002**, *190*, 177−184.
(29) (a) Tashiro, K.; Sasaki, S.; Kobayashi, M. *Macromolecules* **1996**, *29*, 7460−7469. (b) Ungar, G.; Zeng, X.-B. *Chem. Rev.* **2001**, *101*, 4157−4188.
(30) (a) Otocka, E. P.; Kwei, T. K. *Macromolecules* **1968**, *1*, 244−249. (b) Kang, N.; Xu, Y.-Z.; Wu, J.-G.; Feng, W.; Weng, S.-F.; Xu, D.-F. *Phys. Chem. Chem. Phys.* **2000**, *2*, 3627−3630.
(31) The g' values given for the functional copolymers were calculated using the Mark−Houwink parameters for PE and are therefore only approximate (giving rise to values distributed somewhat above and below the theoretical linear value of 1.0), since Mark−Houwink parameters can vary with copolymer composition. However, for materials with similar compositions, *relative* g' comparisons may be used to accurately characterize relative differences in LCB.
(32) (a) Flory, P. J. *J. Chem. Phys.* **1949**, *17*, 223−240. (b) Flory, J. P. *Trans. Faraday Soc.* **1955**, *51*, 848−857.
(33) (a) Isasi, J. R.; Haigh, J. A.; Graham, J. T.; Mandelkern, L.; Alamo, R. G. *Polymer* **2000**, *41*, 8813−8823. (b) Alamo, R. G.; Mandelkern, L. *Thermochim. Acta* **1994**, *238*, 155−201 and references therein. (c) Alamo, R. G.; Domszy, R.; Mandelkern, L. *J. Phys. Chem.* **1984**, *88*, 6587−6595. (d) Alamo, R. G.; Mandelkern, L. *Macromolecules* **1989**, *22*, 1273−1277. (e) Alamo, R. G.; Viers, B. D.; Mandelkern, L. *Macromolecules* **1993**, *26*, 5740−5747. (f) Alizadeh, A.; Richardson, L.; Xu, J.; McCartney, S.; Marand, H.; Cheung, Y. W.; Chum, S. *Macromolecules* **1999**, *32*, 6221−6235.
(34) (a) Gomez, M. A.; Tonelli, A. E.; Lovinger, A. J.; Schilling, F. C.; Cozine, M. H.; Davis, D. D. *Macromolecules* **1989**, *22*, 4441−4451. (b) Bodily, D.; Wunderlich, B. J. *Polym. Sci., Part A-2: Polym. Phys.* **1966**, *4*, 25−40. (c) Ke, B. *J. Polym. Sci.* **1962**, *61*, 47−59. (d) Richardson, M. J.; Flory, P. J.; Jackson, J. B. *Polymer* **1963**, *4*, 221−236. (e) Pérez, E.; VanderHart, D. L. J. *Polym. Sci., Part B: Polym. Phys.* **1987**, *225*, 1637−1653. (f) Wunderlich, B.; Poland, D. *J. Polym. Sci., Part A* **1963**, *1*, 357−372. (g) Baker, C. H.; Mandelkern, L. *Polymer* **1966**, *7*, 7−21. (h) Phillips, P. J.; Wilkes, G. L.; Delf, B. W.; Stein, R. S. *J. Polym. Sci., Part A-2: Polym. Phys.* **1971**, *9*, 499−515.
(35) Sanchez, I. B.; Eby, R. K. *J. Res. Natl. Bur. Stand. (U.S.)* **1973**, *77A*, 353−358.
(36) (a) VanderHart, D. L.; Pérez, E. *Macromolecules* **1986**, *19*, 1902−1909. (b) Kawai, T.; Ujihara, K.; Maeda, H. *Makromol. Chem.* **1970**, *132*, 87−111. (c) Holdsworth, P. J.; Keller, A. *J. Polym. Sci., Part B: Polym. Lett.* **1967**, *5*, 605−612.
(37) (a) Keating, M. Y. *Thermochim. Acta* **1994**, *243*, 129−145. (b) Okui, N.; Kawai, T. *Makromol. Chem.* **1972**, *154*, 161−176. (c) Salyer, I. O.; Kenyon, A. S. *J. Polym. Sci., Part A-1: Polym. Chem.* **1971**, *9*, 3083−3103. (d) Nielsen, L. E. *J. Polym. Sci.* **1960**, *42*, 357−366. (e) Chowdhury, F.; Haigh, J. A.; Mandelkern, L.; Alamo, R. G. *Polym. Bull. (Berlin)* **1998**, *41*, 463−470. (f) Buerger, D. E.; Boyd, R. H. *Macromolecules* **1989**, *22*, 2699−2705. (g) Kortleve, G.; Tuijnman, C. A. F.; Vonk, C. G. *J. Polym. Sci., Part A-2: Polym. Phys.* **1972**, *10*, 123−131. (h) Vonk, C. G. *J. Polym. Sci., Part C: Polym. Symp.* **1972**, *38*, 429−435. (i) Takahashi, M.; Tashiro, K.; Amiya, S. *Macromolecules* **1999**, *32*, 5860−5871. (j) Buerger, D. E.; Boyd, R. H. *Macromolecules* **1989**, *22*, 2694−2699. (k) Otocka, E. P.; Kwei, T. K.; Salovey, R. *Makromol. Chem.* **1969**, *129*, 144−156. (l) MacKnight, W. J.; Taggart, W. P.; McKenna, L. *J. Polym. Sci., Part C: Polym. Symp.* **1974**, *46*, 83−96. (m) Horrion, J.; Agarwal, P. K. *Polym. Commun.* **1989**, *30*, 264−267. (n) Somrang, N.; Nithitanakul, M.; Grady, B. P.; Supaphol, P. *Eur. Polym. J.* **2004**, *40*, 829−838.
(38) (a) Chou, R. T.; Keating, M. Y.; Hughes, L. J. *Annu. Tech. Conf.-Soc. Plast. Eng.* **2002**, *60th* (2), 1832−1836. (b) Gutzler, F.; Wegner, G. *Colloid Polym. Sci.* **1980**, *258*, 776−786.
(39) For the high-CO EVOH materials, it is also possible that a change in the heat of fusion for a perfect crystal from the PE value of 293 J/g towards the value for poly(ethylene-*alt*-CO) distorts the X_c calculation.
(40) Chen, H. Y.; Chum, S. P.; Hiltner, A.; Baer, E. *J. Polym. Sci., Part B: Polym. Phys.* **2001**, *39*, 1578−1593.
(41) In the discussion of DMTA data, some functional group comparisons are made using data obtained in different modes. Although their deformation processes differ (for example, elongation during tensile stress could potentially facilitate functional group interactions), modulus measurements for the two series of ROMP EVOHs (which were taken in different modes) showed reasonably good comparability, as did specific comparative measurements on selected other samples (Tables 2 and 3).
(42) Experimental limitations, including compositional uncertainties for ROMP EAAs and data scatter for the high-melting EVOHs, complicate any close examination of the relative behaviors of the EAA and EVOH copolymers. ROMP EVOHs appeared to have generally higher moduli than ROMP EAAs at all compositions (noting sample **EAA−2.6-R** contains ketone and alcohol groups), while free-radical EVOHs showed similar moduli to free-radical EAAs at low comonomer contents and higher moduli at higher comonomer contents.
(43) Kanekiyo, M.; Kobayashi, M.; Ando, I.; Kurosu, H.; Amiya, S. *Polymer* **2000**, *41*, 2391−2404.

MA070085P